

NEW MODEL TO PREDICT HEAT TRANSFER COEFFICIENT FOR FLOW  
BOILING IN MICROFIN TUBES

By  
Reem Merchant

A THESIS

Submitted in partial fulfillment of the requirements for the degree of

MASTER OF SCIENCE

In Mechanical Engineering

MICHIGAN TECHNOLOGICAL UNIVERSITY

2016

© 2016 Reem Merchant

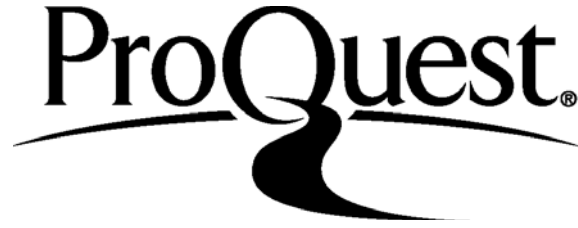
ProQuest Number: 10168471

All rights reserved

INFORMATION TO ALL USERS

The quality of this reproduction is dependent upon the quality of the copy submitted.

In the unlikely event that the author did not send a complete manuscript and there are missing pages, these will be noted. Also, if material had to be removed, a note will indicate the deletion.



ProQuest 10168471

Published by ProQuest LLC (2016). Copyright of the Dissertation is held by the Author.

All rights reserved.

This work is protected against unauthorized copying under Title 17, United States Code  
Microform Edition © ProQuest LLC.

ProQuest LLC.  
789 East Eisenhower Parkway  
P.O. Box 1346  
Ann Arbor, MI 48106 - 1346



This thesis has been approved in partial fulfillment of the requirements for the Degree of MASTER OF SCIENCE in Mechanical Engineering.

Department of Mechanical Engineering-Engineering Mechanics

Thesis Co-Advisor: *Dr. Sunil Mehendale*

Thesis Co-Advisor: *Dr. V.C. Rao Komaravolu*

Committee Member: *Dr. Mahdi Shahbakhti.*

Department Chair: *Dr. William Predebon*



## Table of contents

List of figures.....	vii
List of tables.....	ix
Nomenclature.....	x
Preface.....	xiii
Acknowledgments .....	xiv
Abstract.....	xv
1. Overview.....	1
1.1. Key findings.....	1
1.2. Introduction and background.....	3
2. Survey of selected flow boiling correlations.....	7
2.1. Yu et al. (1995) .....	11
2.2. Thome et al. (1997) .....	14
2.3. Cavallini et al. (1999) .....	17
2.4. Yun et al. (2002) .....	21
2.5. Chamra and Mago (2007) .....	23
2.6. Hamilton et al. (2008) .....	24
2.7. Wu et al. (2013) .....	26
3. Experimental flow boiling HTC data.....	28
4. New model to predict flow boiling HTCs in microfin tubes.....	34
5. Results and discussion.....	44
5.1. Global evaluation of new model.....	44
5.2. Application-specific evaluation of new model.....	50
6. Conclusions and recommendations for future research.....	60
References.....	61
Appendix A.....	69



## List of figures

1.	2.1.	Basic geometry of microfin tubes .....	3
	2.2.	Critical factors affecting flow boiling in microfin tubes.....	4
3.	1.	Graph showing the variation of MAD and SD against X30% for experimental references in published literature .....	33
4.	1.	Property plot of density ratio vs. saturation temperature for different refrigerants.....	38
	2.	Property plot of viscosity ratio vs. saturation temperature for different refrigerants.....	38
	3.	Property plot of thermal conductivity vs. saturation temperature for different refrigerants.....	39
	4.	Property plot of enthalpy of vaporization vs. saturation temperature for different refrigerants.....	39
	5.	Property plot of surface tension vs. saturation temperature for different refrigerants.....	40
5.	1.1.	Scatter plots of predicted HTC vs. experimental HTC .....	46
	1.2.	X30% values for each dataset division for deriving constants to select the best model to predict flow boiling HTCs for microfin tubes.....	49
	2.1.	Comparison of trends for specific applications [ $\text{CO}_2$ , $T_{\text{sat}}=5^\circ\text{C}$ , $d_r=4.4\text{mm}$ , $G=424\text{kg/m}^2\text{s}$ , $q=12000\text{W/m}^2$ ] for linearized model and best among existing models .....	52
	2.2.	Comparison of trends for specific applications [ $\text{CO}_2$ , $T_{\text{sat}}=0^\circ\text{C}$ , $d_r=4.4\text{mm}$ , $G=424\text{kg/m}^2\text{s}$ , $q=5000\text{W/m}^2$ ] for linearized model and best among existing models .....	52
	2.3.	Comparison of trends for specific applications [ $\text{NH}_3$ , $T_{\text{sat}}=-20^\circ\text{C}$ , $d_r=11.13\text{mm}$ , $G=100\text{kg/m}^2\text{s}$ , $q=50000\text{W/m}^2$ ] for linearized model and best among existing models .....	54
	2.4.	Comparison of trends for specific applications [ $\text{R32}$ , $T_{\text{sat}}=-9.878^\circ\text{C}$ , $d_r=5.37\text{mm}$ , $G=150\text{kg/m}^2\text{s}$ , $q=15000\text{W/m}^2$ ] for linearized model and best among existing models .....	56
	2.5.	Comparison of trends for specific applications [ $\text{R22}$ , $T_{\text{sat}}=22^\circ\text{C}$ , $d_r=14.13\text{mm}$ , $G=205\text{kg/m}^2\text{s}$ , $q=14200\text{W/m}^2$ ] for linearized model and best among existing models .....	56
	2.6.	Comparison of trends for specific applications [ $\text{R407C}$ , $T_{\text{sat}}=-10^\circ\text{C}$ , $d_r=8.95\text{mm}$ , $G=300\text{kg/m}^2\text{s}$ , $q=20000\text{W/m}^2$ ] for linearized model and best among existing models .....	57



2.7.	Comparison of trends for specific applications [R134a, $T_{\text{sat}}=-14.5^{\circ}\text{C}$ , $d_r=8.92\text{mm}$ , $G=53\text{kg/m}^2\text{s}$ , $q=2100\text{W/m}^2$ ] for linearized model and best among existing models.....	57
A.	1. Applications studied for Carbon Dioxide .....	69
	2. Applications studied for Ammonia .....	69
	3 Applications studied for Halogenated refrigerants (pure).....	70
	4 Applications studied for Halogenated refrigerants (mixed)...	70

## List of tables

2.	1.	Limitations in existing flow boiling HTC models.....	7
	3.1	Table of constants used in Cavallini et al. (1999) .....	17
	5.1	Table of constants used in Chamra and Mago (2007).....	23
3.	1	Experimental database summary – Refrigerant properties and no. of data points.....	29
	2	Experimental database summary – Operating conditions ....	31
	3	Experimental database summary – Geometric conditions....	32
4.	1	Constants to be used in the linearized model for different categories.....	43
5.	1.1	MD comparison.....	44
	1.2	MAD comparison.....	44
	1.3	SD comparison.....	45
	1.4	X30% comparison.....	45
	1.5	Dataset divisions for deriving constants to select the best model to predict flow boiling HTCs for microfin tubes.....	48
	2.1	Specific applications studied for CO <sub>2</sub> .....	51
	2.2	Specific applications studied for NH <sub>3</sub> .....	53
	2.3	Specific applications studied for Halogenated refrigerants...	55
	2.4	Comparison of X30% for modified Wu et al. (2013) and new model.....	58

## Nomenclature

Regular text

A	total inner surface heat transfer area of a micro fin tube, $m^2$
$A_c$	cross sectional area, $m^2$
Avg	Average
Bo	Bond number
Co	convection number
D	diameter, m
$E_{rb}$	convective boiling enhancement factor
F	fanning friction factor
Fr	Froude number
G	mass flux, $kg/m^2-s$
G	acceleration due to gravity, $m/s^2$
H	fin height, m
$H_{fg}$	latent heat of vaporization, J/kg
HTC	heat transfer coefficient $W/(m^2K)$
K	thermal conductivity, $W/m-K$
M	molar mass, $kg/mol$
MD	Mean deviation
MAD	Mean absolute deviation
SD	Standard deviation
N	total number of points in the given dataset
$n_g$	number of fins
Nu	Nusselt number

P	pressure, Pa
P	axial pitch, m
Pr	Prandtl number
P	reduced pressure
q	heat flux, W/ m <sup>2</sup>
r	bubble radius, m
Re	Reynolds number
Rx	geometry enhancement factor
S	nucleate boiling suppression factor
T	temperature, °C
x	vapor quality
X30%	percentage number of points between ± 30 % deviation lines
X <sub>tt</sub>	Lockhart - Martinelli parameter

#### Greek letters

$\alpha$	heat transfer coefficient, W/m <sup>2</sup> -K
$\beta$	helix angle of the fin, °
$\delta$	film thickness, m
$\varepsilon$	void fraction
$\vartheta$	specific volume, m <sup>3</sup> /kg
$\mu$	dynamic viscosity, Pa-s
$\rho$	density, kg/m <sup>3</sup>
$\gamma$	apex angle of the fin, °

## Subscripts

b	departure bubble
cooper	HTC base term as defined in Cavallini et al. (1999)
crit	critical
cv	convective boiling
go	gas only
h	hydraulic
i	fin tip diameter
l	liquid state
lo	liquid only
mf	microfin
nb	nucleate boiling
onb	onset of nucleate boiling
pb	pool boiling
red	reduced
r	inner root
sat	saturation
tp	two-phase
v	vapor state
w	wall

## **Preface**

This thesis is submitted in partial fulfilment of the requirements for a Degree of Master of Science in Mechanical Engineering. All work presented in this thesis is done largely by Ms. Reem Merchant under the guidance of Dr. Sunil Mehendale. In this thesis, relevant citations have been provided for research conducted by other authors.

## Acknowledgements

This thesis would not have been possible without the mentorship of my advisor, Dr. Sunil Mehendale. He has used his extensive industry experience to identify problems faced by practicing engineers and has given direction and rigor to this thesis. His guidance has been very valuable throughout the course of this research and has also contributed towards my successful completion of M.S. degree. Dr. Sunil Mehendale and his family – Mrs. Madhura Mehendale, Mihir Mehendale and Soham Mehendale have supported me emotionally and have become my family. I would like to extend my warmest gratitude to them all.

I am grateful to Dr. Mark Gockenbach, for helping me in the process of MATLAB coding and understanding the statistics involved in the research. I would also like to thank him for sharing his MATLAB code for the non-linear regression which helped complete this research in a timely manner. His expertise and guidance has been very useful in this study. His willingness to teach and help with this research has helped to understand the data and results obtained.

I would like to thank Dr. Yeonwoo Rho for sharing her insights about the R software.

I would like to extend appreciation towards Dr. K.V.C. Rao for being co-advisor and part of my defense committee. His backing has contributed towards the completion of this thesis.

I am thankful to Dr. Mahdi Shahbakhti for agreeing to be a part of my defense committee and for his support.

Special thanks to my friends, especially Mr. Apurva Baruah for helping me with the R software analysis.

I am grateful to my parents, for their unconditional love and unceasing encouragement.

## Abstract

Microfin tubes are used extensively in the HVAC&R applications. Rigorous government regulations and escalating raw material costs demand higher heat transfer coefficients (HTCs) and hence better performance for practical applications. Hence, engineers are constantly trying to improve the performance of thermal systems. With introduction of smaller tubes and newer refrigerants, a lot of tests need to be conducted in the industry. Accurate mathematical modeling can significantly reduce the time and cost of experimentations. Currently, there are many existing models in published literature for predicting the flow boiling HTCs in microfin tubes. However, these models are not accurate enough and the practicing engineer does not have specific guidelines as to which model should be used for a given application. The objective of this research is to propose a new linearized model for predicting HTCs for flow boiling in horizontal microfin tubes. The constants for this new linearized model are based on 2201 experimental data points collected from existing literature spanning a wide range of refrigerants, geometric and operating parameters. In addition, specific recommendations have been provided to give the practicing engineer guidelines for assessing the applicability of the new model as well as existing models.





# 1. Overview

## 1.1. Key findings

Many mathematical models have been proposed to predict the flow boiling heat transfer coefficients (HTCs) in microfin tubes. These mathematical models cannot predict HTCs for the entire range of parameters that is used in the industry. This is because the models are based on limited experimentation and the database is not comprehensive. Hence, these models cannot be used to predict HTCs over the entire range of geometric and operating parameters. The literature where the models are reported, propose that the HTCs can be predicted within  $\pm 30\%$  for almost 70-80% of the all points considered. Thus, the existing models propose good overall predictions, but they cannot be applied to specific sets of geometric and operating parameters over the entire range of ranges used in the industry. The current work focuses on developing a new validated model that can be confidently applied to specific ranges of geometric and operating parameters, i.e., to specific industrial applications. Following are the novel contributions of this research

- The database of experimental points used to develop the model is comprehensive and up-to-date, consisting of 2,201 points spanning a wide range of refrigerants (CO<sub>2</sub>, NH<sub>3</sub>, pure and mixed halogenated refrigerants), operating (vapor quality, heat and mass flux) and geometric parameters (diameter, fin height, no. of fins, helix and apex angles).
- A new model based on key dimensionless parameters that govern the physics of the flow boiling process in microfin tubes was developed and validated. The predictions of the

model were compared to those of existing popular seven correlations.

- X30% which is a more intuitive and ‘visual’ metric to assess the applicability of the correlation was used through this research in addition to the traditionally used MD, MAD and SD.
- The entire database was split into different categories such as low and high heat flux, mass flux and diameters and also based on refrigerants. These different subsets were compared for performance against existing models to give application-specific guidelines.
- This research shows that the global metrics, that are based on MD, MAD, SD and X30% for the full experimental database does not give sufficient insight into particular industrial applications. Hence, 45 individual subsets were extracted from the full database for a single refrigerant, particular diameter, heat and mass flux for varying quality. The 45 individual trend studies for these subsets of data were analyzed to provide application-specific guidelines.

## 1.2. Introduction and background

Microfin tubes were first developed in Japan (Fujie et al. (1977)). These tubes started gaining popularity in the HVAC&R industry in the 1980s. Since then microfin tubes are widely used due to their superior heat transfer characteristics (HTCs). Microfin tubes can provide HTCs of almost 1.00 to 3.00 times those in an equivalent smooth tube, while the pressure drop can be 1.20 to 2.00 times the pressure drop in a corresponding smooth tube (Dang et al. (2010)). Due to this thermal performance benefit, microfin tubes are widely used in the HVAC&R industry. There are various kinds of internally finned tubes used in the industry such as herringbone tube, crossed grooved tubes etc. However, for the current study only single helical finned tubes are considered. Typical geometry of microfin tubes is shown in Figure 1.2.1. Microfin tubes are made by creating an interference fit between tubes and fins using a mandrel. This mechanical process decreases the thermal contact resistance (Mehendale (2013)).

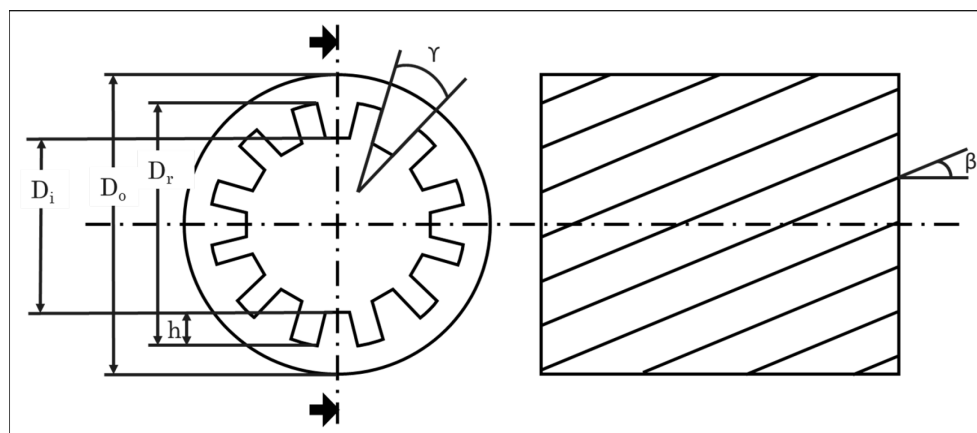


Figure 1.2.1. Basic geometry of microfin tubes

Flow boiling in microfin tubes has been widely studied and there are a large number of published articles. Many correlations have been proposed to predict the flow boiling HTC in microfin tubes. Some of the popular correlations are Cavallini et al. (1999), Thome et al. (1997) and Wu et al. (2013). In addition, many experiments have been conducted to study HTCs for flow boiling in microfin tubes. These experiments have been conducted for a various refrigerants spanning a wide range of geometric and operating parameters. Geometric parameters include tube diameter, fin height, helix angle, apex angle and number of fins etc. while operating parameters include mass flux, heat flux, quality etc. Flow boiling in microfin tubes involves the complex interplay of many parameters as shown in Figure 1.2.2.

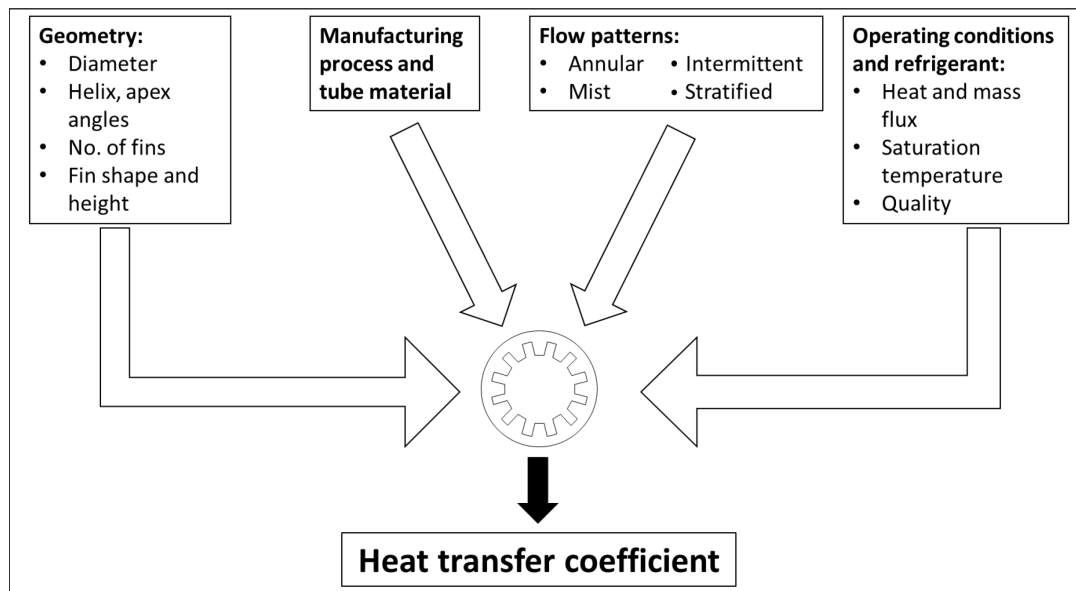


Figure 1.2.2. Critical factors affecting flow boiling in microfin tubes

Due to the complex interactions between these parameters, no single correlation can accurately predict the HTC across a wide range of geometric and operating parameters that are used in the industry. The industry is looking towards new refrigerants and increasingly smaller tubes diameters to cope with increasing regulatory pressures for higher thermal efficiency. Due to the lack of a single good correlation, the only alternative is to test the tubes for a wide range of operating conditions, which is time-consuming and costly.

Due to the complexity of flow boiling in microfin tubes, the existing correlations are either empirical or semi-empirical in nature. Merchant and Mehendale (2015) have given general guidelines for selecting the best available correlation from existing correlations for a given application. As per the recommendations of Merchant and Mehendale (2015) for halogenated refrigerants with tube diameter greater than 5 mm, Cavallini et al. (1999) model can be used to best predict the flow boiling HTC in microfin tubes. Similarly, Thome et al. (1997) model can be used for carbon dioxide (CO<sub>2</sub>) flowing in tube diameters greater than 5 mm, while Wu et al. (2013) model can be used for both halogenated and CO<sub>2</sub> refrigerants in tube diameters less than 5 mm.

In the published literature there are many models that can be used to predict flow boiling HTCs. However, there are no specific guidelines as to which correlation should be used to predict flow boiling HTC for any given industrial application. Hence the practicing engineer does not know which model should be used. Also, it is seen that a single model cannot predict all experimental data ranges that are used in the industry. Hence, it is important to have a model that can be used for a wide range of experimental data. The

current work proposes a linearized model to predict flow boiling HTC in microfin tubes. This model is proposed to be applicable across a wide range of geometric and operating parameters. In addition, recommendations have been provided to use correlation with different set of constants for different experimental data ranges. This ensures that the linearized model works well over the wide range of experimental data.

## 2. Survey of selected flow boiling correlations

Flow boiling in smooth tubes is based on two main mechanisms of heat transfer: nucleate and convective boiling. The interplay of these two parameters depends on variables such as mass flux, heat flux, saturation temperature, vapor quality and tube surface roughness. In horizontal smooth tubes, the two phase flow is affected by gravity which results in asymmetric distribution of the liquid and gas phase, especially at low mass flux. At very low heat flux, convection is the main mode of heat transfer. As heat flux increases, nucleation or bubble formation begins to occur. The numerous discrete bubbles formed in the liquid phase travel to the upper side of the tube. Such flow is also called bubbly flow. At high mass velocity, bubbly flow is observed. As the vapor quality increases, due to gravity, there is a clear distinction between the liquid phase in the bottom side of the tube and the vapor phase in the upper side of the tube. This is the stratified flow regime. Further as vapor quality increases, the liquid form waves which sweep the upper surface of the tube. This is the intermittent flow. Eventually, as the liquid becomes equally distributed around the inner periphery of the tube, annular flow regime occurs. Annular flows have a liquid periphery surrounding a vapor core. Due to gravity, at low mass flux, the thickness of this liquid film is uneven at the top and bottom of the smooth tube. If helical microfins are present on the inner side of the tube, then the liquid in the lower region of the tube is lifted to the top and swirled due to capillary effect. This increases the thermal performance of the microfin tubes compared to the smooth tubes.



In published literature, many authors have proposed models to calculate the flow boiling HTC in microfin tubes. Seven existing correlations were studied - Yu et al. (1995), Cavallini et al. (1999), Thome et al. (1997), Hamilton et al. (2008), Yun et al. (2002), Chamra and Mago (2007) and Wu et al. (2013). The choice of these seven models was based on high number of citations and basic physics that are applied to the equations. The basic physics that these models include consists of separate terms capturing the flow physics and empirical constants from a wide range of experimental data. However, existing models do not capture an encompassing database that is of current use in industry today. Limitations of the existing models is given in Table 2.1. Detailed description of the models can be found in the paragraphs below.

Table 2.1. Limitations in existing flow boiling HTC models

<b>Model</b>	<b>No. of experimental runs</b>	<b>Limitations</b>
Yu et al. (1995)	150	No data for CO <sub>2</sub> and NH <sub>3</sub> . No data for tubes less than 5 mm diameter.
Thome et al. (1997)	Not available	No data for tubes less than 5 mm diameter.
Cavallini et al. (1999)	110	No data for CO <sub>2</sub> and NH <sub>3</sub> . No data for tubes less than 5 mm diameter.
Yun et al. (2002)	749	No data for CO <sub>2</sub> and NH <sub>3</sub> . No data for tubes less than 5 mm diameter. Model presented does not have terms to account of effect of key geometric parameter like helix angle.
Chamra and Mago (2007)	380	No data for CO <sub>2</sub> and NH <sub>3</sub> . No data for tubes less than 5 mm diameter.
Hamilton et al. (2008)	6360	No data for CO <sub>2</sub> and NH <sub>3</sub> . No data for tubes less than 5 mm diameter.
Wu et al. (2013)	503	No data for NH <sub>3</sub> .

## ***Statistical quantities – definition and use***

The existing seven correlations – Cavallini et al. (1999), Wu et al. (2013), Thome et al. (1997), Yu et al. (1995), Yun et al. (2002), Chamra and Mago (2007) and Hamilton et al. (2008) were modelled using EES (Engineering equation solver) (Copyright F-Chart Software). The correlations were validated using the data from Padovan (Thesis: Università Degli Studi Di Padova). This validation procedure was carried out to ensure that the correlations are accurate and no manual errors are made while modelling. This increases the confidence of the reported results.

In already existing literature, the predictive performance of correlations is normally measured using statistical quantities like MD, MAD and SD. The equations used to calculate these statistical quantities are given below.

$$error\% = \frac{HTC_{pred} - HTC_{expt}}{HTC_{expt}} \times 100 \quad (2.1)$$

$$MD = \frac{\sum_{i=1}^n error\%}{n} \quad (2.2)$$

$$MAD = \frac{\sum_{i=1}^n |error\%|}{n} \quad (2.3)$$

$$SD = \sqrt{\frac{\sum_{i=1}^n (error\% - MD)^2}{n-1}} \quad (2.4)$$

MD and MAD measure the deviation from a central value while SD gives the scatter of the data. These statistical quantities are based on average number of points about a central value. If equal magnitude of data is scattered over either sides of this central value, then the value of MD reported is very small and is misleading. Even if the MD reported is low, the scatter may be large. MD can represent if the data is over-predicted or under-predicted in general. MAD is similar to the concept of MD; the only difference is that the absolute

value of the errors is considered to calculate MAD. MAD can show if the data is centered properly but cannot represent the scatter about the central value. SD reports the scatter and cannot define the magnitude of the scatter of the different points clearly. Hence, the existing methods of representing the data statistically is not sufficient by itself. In the current work and from work based on Merchant and Mehendale (2015), the term X30% is given. X30% is defined in the equation below.

$$X30\% = \frac{\text{no.of points between } \pm 30\% \text{ lines}}{\text{total no.of points}} \times 100 \quad (2.5)$$

It is the number of points within  $\pm 30\%$  lines. This quantity is not new in statistics. However, it has not been used before for measuring the predictive performance of HTC. The value  $\pm 30\%$  is a wide range to be considered for error in many conventional cases. However, as shown in Figure 1.2.2, there is an interplay of many factors involved in predicting the HTC in microfin tubes. Due to this complexity, the flow boiling in microfin tubes is very unstable to predict dry-out. The dry-out point can vary up to 10% of the surface area of the microfin tube (Wedekind (1965)). Hence, if predictions of HTC come within  $\pm 30\%$  of the experimentally determined values, then it is considered as satisfactory. The introduction of the X30% variable in the research related to predicting HTCs in microfin tubes will make sense, intuitively and visually, to practicing engineers. X30% can combine the concepts of MAD and SD giving a better visualization and predicting scatter and deviation of the points.

## 2.1. Yu et al. (1995)

Yu et al. (1995) conducted flow boiling experiments using copper microfin tubes of inner diameter 8.37 mm. Pure refrigerants were used - R134a, R22 and R123. The test section was heated using water jacket in parallel and counter flow conditions. The experimental data did not conform with the correlations proposed by Kandlikar (1991), Miyara et al. (1988), Kido-Uehara (1994) and Murata-Hashizume (1993), hence Yu et al. (1999) proposed an additive model for wavy-annular and annular flow regimes. This additive model was based on Takamatsu et al. (1993). The proposed model and the experimental data agreed with MAD of 12%. The MAD is the average of the absolute values of the relative errors measured from the experimental values.

Yu et al. (1995) is an additive model which simply accounts for the effect of nucleate and convective boiling mechanisms by addition of the terms.

$$HTC = HTC_{nb} + HTC_{cv} \quad (2.1.1)$$

The pool boiling (pb) term is suitably modified by using a suppression factor and ‘constant’ that depends on ‘n’ which is the ratio of the convective HTC to the suppressed pool boiling HTC. In regular pool boiling, that is, where there is no forced convection, the bubbles are formed at nucleation sites and these bubbles then begin to grow with increasing heat flux. At a particular heat flux, also called onset of nucleate boiling, these bubbles depart from the surface and travel through the liquid. This upward movement of the bubble causes agitation of the fluid and leads to natural convection. However, when there is forced convection, the bubble formation process is disturbed. The bubbles are formed at

nucleation sites but are carried away by the flow as soon as they reach a particular size depending on the mass flux. This leads to a phenomenon called suppression of pool boiling. Hence, the term ‘S’ is required to account for these suppression effects.

$$HTC_{nb} = \text{constant } HTC_{pb}S \quad (2.1.2)$$

$$\text{constant} = \frac{1}{1+0.875n+0.518n^2-0.159n^3+0.7907n^4} \quad (2.1.3)$$

$$n = \frac{HTC_{cv}}{HTC_{pb}S} \quad (2.1.4)$$

The following expression for ‘S’ gives the nucleate boiling suppression factor for forced convective boiling where  $D_b$  represents the thickness of bubble growth region. The term  $\xi$  gives the Nusselt number enhancement due to convection. The term S represents the suppression of pool boiling due to the enhancement caused by convection.

$$S = \frac{1}{\xi(1-\exp(-\xi))} \quad (2.1.5)$$

$$\xi = D_b h_{cv} / k_l \quad (2.1.6)$$

The term  $\left[\frac{2\sigma}{g(\rho_l-\rho_v)}\right]^{0.5}$  is defined as the Laplace constant and the physical significance is that it gives characteristic length of the bubble layer. It involves the effect of surface tension and buoyancy effect. The term  $\frac{c_{pl}}{h_{fg}} T_{sat}$  is the modified Jacob number which is included to account for the ratio of sensible to latent energy absorbed during phase change. The multiplication of this term with the density ratio is to make the effect of pressure more pronounced.

$$D_b = 10^{-5} \left[\frac{\rho_l c_{pl}}{\rho_v h_{fg}} T_{sat}\right]^{1.25} \left[\frac{2\sigma}{g(\rho_l-\rho_v)}\right]^{0.5} \quad (2.1.7)$$

The two-phase Reynolds number is obtained by modifying the liquid-phase Reynolds number using a factor involving the Lockhart-Martinelli parameter. Two-phase flow is distinguished from single-phase flow primarily by the terms vapor quality, density and viscosity ratios. Single-phase or liquid/gas-only pressure drop can be easily calculated using the Blasius equation or Moody diagram. However, for two phase pressure drop this liquid/gas-only pressure drop term needs to be modified by multiplying it with a suitable factor, which is a function of  $X_{tt}$ . This term  $X_{tt}$  consists of the vapor quality, density and viscosity ratios which determines the differentiating conditions between the liquid-only and two phase-flow term.

$$Re_{tp} = Re_l F^{1/0.8} \quad (2.1.8)$$

$$F = 1 + 2 \left[ \frac{1}{X_{tt}} \right]^{-0.88} + 0.8 \left[ \frac{1}{X_{tt}} \right]^{1.03} \quad (2.1.9)$$

$$Re_l = G d_i / \mu_l \quad (2.1.10)$$

$$X_{tt} = \left( \left( \frac{1-x}{x} \right)^{0.9} \left( \frac{\rho_g}{\rho_l} \right)^{0.5} \left( \frac{\mu_g}{\mu_l} \right)^{0.1} \right) \quad (2.1.11)$$

The convective Nusselt number ( $Nu_{cv} = HTC_{cv} d_i / k_l$ ) is calculated using the two-phase Reynolds number and liquid-only Prandtl number. The following equation is a form of the Dittus-Boelter equation for internal turbulent flow where the constants 0.028 and 0.8 are calculated using regression. The exponent for  $Pr_l$  is 0.4 which for heating, that is, when the wall is hotter than the bulk fluid.

$$HTC_{cv} = 0.028 Re_{tp}^{0.8} Pr_l^{0.4} \frac{k_l}{d_i} \quad (2.1.12)$$

## 2.2. Thome et al. (1997)

Thome et al. (1997) conducted annular flow boiling experiments using R123, R134a, R404A, R402A, R502, CO<sub>2</sub> for vapor qualities from 15-80 %, mass flux 100-500 kg/m<sup>2</sup>-s and heat flux from 2 -47 kW/m<sup>2</sup>. For this data the authors proposed an asymptotic model. The nucleate and convective boiling terms were modelled using Cooper (1984) and Kattan et al. (1998) respectively. Cooper (1984) suggests a nucleate pool boiling equation for pure refrigerants which is based on the total heat flux and effective internal surface area. Kattan et al. (1998) based the convective boiling term for plain tubes using annular turbulent film model. Padovan (Thesis: Università Degli Studi Di Padova) reports that HTC predicted by Thome et al. (1997) was found to be independent of saturation pressure. Also, as reported by Padovan (Thesis: Università Degli Studi Di Padova), HTC increases with vapor quality due to the effect of the enhanced nucleate boiling component in the predicted HTC value. This finding is also confirmed in this work as well.

$$HTC = E_{mf} (HTC_{nb}^3 + HTC_{cv}^3)^{1/3} \quad (2.2.1)$$

To comprehend the effect of refrigerant mass flux on HTC, Thome et al. (1997) proposed a semi-empirical polynomial function for  $E_{mf}$ .

$$E_{mf} = 1.89 (G/500)^2 - 3.7 (G/500) + 3.02 \quad (2.2.2)$$

The nucleate boiling component depends on the heat flux, as at very low heat flux the nucleate component is almost zero. This is captured by the following nucleate boiling HTC terms.

$$HTC_{nb} = 55 P_R^{0.12} (-\log_{10}(P_R))^{-0.55} M^{-0.5} q^{0.67} \quad (2.2.3)$$

The nucleate boiling term also contains the effect of the  $P_R$  (reduced pressure). This reduced pressure is the ratio of the saturation to critical pressure. This pressure ratio would capture the effect of nucleation bubbles formed and its motion from the base of the tube towards the upper side. A bubble is formed within the liquid when a certain pressure is reached inside the bubble. This bubble then grows in size as pressure inside the bubble increases. When the bubble reaches a certain size the bubble departs from the surface and moves to the surface of the liquid. Hence pressure plays a critical role in bubble formation. If the surrounding pressure is high, then the bubble would collapse and nucleation would start at a later stage in boiling, that is, when the heat flux is high. The heat flux should be the critical heat flux at which the onset of nucleate boiling begins. The rate of bubble formation and flux at which these bubbles are formed depends on the refrigerant in use. This nucleation process also depends on the refrigerant property and hence the molar mass ( $M$ ) term is also used in the nucleate boiling term.

The smooth tube convective boiling term is modified using  $E_{rb}$  term as the microfins enhance the liquid-only HTC increasing the two phase convective contribution.  $E_{rb}$  term captures the effect of the fin height, fin pitch, root diameter and helix angle of the microfin tubes. The terms  $Re_l$  and  $Pr_l$  appear twice in the  $HTC_{cv}$  term, that is, in  $E_{rb}$  and  $HTC_{cv,smooth}$ . This repetition of terms can be avoided as it results in statistical unreliability for regression calculation of the constants.

$$HTC_{cv} = E_{rb} HTC_{cv,smooth} \quad (2.2.4)$$

$$E_{rb} = \left( 1 + (2.64 Re_l^{0.036} Pr_l^{-0.024} (h/d_r)^{0.212} (P/d_r)^{-0.21} (\beta/90)^{0.29} )^7 \right)^{1/7} \quad (2.2.5)$$



The pitch that gives the density of the microfins determines the strength of the capillary effect. The more the density of the fins will mean that there is lesser space between two fins, hence the capillary effect is stronger.

$$p = \pi d_i / n_g \quad (2.2.6)$$

Similar to the Yu et al. (1995) correlation, the smooth tube convective boiling term is calculated from equation which has a functional form similar to the Dittus-Boelter equation for heating. The difference is that the Dittus-Boelter equation is based on the diameter while the modified expression given by Kattan et al. (1998c) depends on the annular film thickness  $\delta$ . This  $\delta$  term is calculated by a geometrical relationship using the root diameter of the microfin tube and void fraction term. The void fraction represents the fraction of the cross sectional area that is occupied by the gas phase.

$$HTC_{cv,smooth} = 0.0133 Re_l^{0.69} Pr_l^{0.4} \frac{k_l}{\delta} \quad (2.2.7)$$

$$Re_l = G d_i / \mu_l \quad (2.2.8)$$

$$\delta = d_r \frac{1-\varepsilon}{4} \quad (2.2.9)$$

The void fraction is determined using the Rouhani and Axelsson (1970) correlation where  $\delta$  is the local thickness of the annular liquid film. Void fraction is the fraction of the cross-sectional area which is occupied by vapor.

$$\varepsilon = \left( \frac{x}{\rho_v} \right) \left( (1 + 0.12(1 - x)) \left( \frac{x}{\rho_v} + \frac{1-x}{\rho_l} \right) + 1.18(1 - x) \frac{(g \sigma (\rho_l - \rho_v))^{0.25}}{G \rho_l^{0.5}} \right)^{-1} \quad (2.2.10)$$

### 2.3. Cavallini et al. (1999)

Cavallini et al. (1999) used an additive model to predict the flow boiling HTC for pure and zeotropic refrigerants like R32/R134a and R407C. MAD of the 110 experimental data points was found to be 21%. The nine constants used were obtained using regression analysis.

Table 2.3.1. Table of constants as used in Cavallini et al. (1999)

	A	B	C	S	T	V	Z
$G < 500 \text{ kg/m}^2\text{s}$	1.36	0.36	0.38	2.14	-0.15	0.59	0.36
$G \geq 500 \text{ kg/m}^2\text{s}$					-0.21		

HTC predictions reported by Cavallini et al. (1999) are shown to be convective boiling dominated at low heat fluxes. The additive model consisted of the convective and nucleate boiling term.

$$HTC = HTC_{nb} + HTC_{cb} \quad (2.3.1)$$

The nucleate boiling term was modified using the suppression factor consisting of the Lockhart-Martinelli parameter. As explained in Yu et al. (1995) the suppression term is captured by a function of the Lockhart-Martinelli parameter. This function is inversely proportional to the convective heat transfer coefficient. However, in Cavallini et al. (1999) the suppression factor is an empirical function of the Lockhart-Martinelli parameter.

$$HTC_{nb} = HTC_{Cooper} S F_1 \quad (2.3.2)$$

$$S = A X t t^B \quad (2.3.3)$$

$$X_{tt} = \left(\frac{1-x}{x}\right)^{0.9} \left(\frac{\rho_g}{\rho_l}\right)^{0.5} \left(\frac{\mu_g}{\mu_l}\right)^{0.1} \quad (2.3.4)$$

$$HTC_{Cooper} = C_{Cooper} P_R^{0.12} (-\log_{10}(P_R))^{-0.55} M^{-0.5} q^{0.67} \quad (2.3.5)$$

$$Pr_l = \mu_l c_{pl} / k_l \quad (2.3.6)$$

$$u_{go} = G / \rho_g \quad (2.3.7)$$

The subscript ‘go’ represents the property if all the liquid in the tube is instantly replaced with gas only. However, the subscript ‘g’ indicates the property if the phase change is occurred and all liquid gets converted into gas. The term  $u_{go}$  gives the superficial velocity that is calculated with only gas inside the tube. This is if all the liquid inside the tube is replaced at that instant with gas phase.

$Nu_{cb,smooth}$  is the product of the all liquid Nusselt number calculated from the Dittus-Boelter correlation for condensation (exponent of  $Pr_l$  is 1/3 for condensation) and the two-phase multiplier term. Cavallini et al. (1999) based his work on prior work done on condensation, hence the Dittus-Boelter correlation for condensation was carried over with exponent of  $Pr_l$  as 1/3. This is a drawback of the Cavallini et al. (1999) model for evaporation.

$$Nu_{cb,smooth} = (0.023 (G d_i / \mu_l)^{0.8} Pr_l^{1/3}) \left( \left( (1-x) + 2.63 x (\rho_l / \rho_g)^{0.5} \right)^{0.8} \right) \quad (2.3.8)$$

The convective HTC term was modified from the two phase smooth convective boiling term. This term was proposed by Cavallini et al. (1999) based on prior work in the condensation field for cross grooved, low finned microfin tubes. Area enhancement factor ( $R_x$ ) is used to capture the effect of the microfins. The microfins result in providing extra wetted area per unit length of the tube.

$$HTC_{cb} d_i/k_l = Nu_{cb,smooth} Rx^{S1} (Bo \cdot Fr)^T F_2 F_3 \quad (2.3.9)$$

Physical significance of the geometrically derived Rx term is to calculate the area enhancement caused due to the presence of microfins. This term captures the effect of microfins and also the shape of the microfins by having the terms of helix and apex angles. This term, Rx, also features in the new model proposed in this work. Froude number (Fr) gives the ratio of inertial force to the gravitational force. The Bond number (Bo) accounts for the effect of gravity force to surface tension.

$$Rx = \frac{\frac{2 h n_g (1 - \sin(\gamma/2))}{\pi d_i \cos(\gamma/2)} + 1}{\cos(\beta)} \quad (2.3.10)$$

$$Fr = \frac{u_g o^2}{g d_i} \quad (2.3.11)$$

$$Bo = \frac{g \rho_l h \pi d_i}{8 \sigma n_g} \quad (2.3.12)$$

The terms F<sub>1</sub>, F<sub>2</sub> and F<sub>3</sub> are normalizing parameters based on the prior work done on condensation. d<sub>o</sub> is given as 0.01m and G<sub>o</sub> is 100 kg/m<sup>2</sup>s according to Cavallini et al. (1999).

$$F_1 = (d_o/d_i)^C \quad (2.3.13)$$

$$F_2 = (d_o/d_i)^V \quad (2.3.14)$$

$$F_3 = (G_o/G)^Z \quad (2.3.15)$$

Cavallini et al. (1999) also proposed a model for mixtures. For the mixture model – especially zeotropes, since there is not a fixed saturation temperature, the saturation pressure is used to find properties like density, specific heats etc. For zeotropes, the liquid vaporizes differentially with the more volatile components evaporating first. This creates a difference in the temperature of the local bubble formation.

$$\alpha = \frac{Q}{(T_w - T_b)(\pi d_i L)} \quad (2.3.16)$$

Also more heat is required to boil the liquid along the tube, if the pressure drop is not too high.  $\alpha_f$  is the HTC of the liquid film while  $\alpha_g$  is the convective HTC of the vapor phase only calculated at mean quality.  $\beta_l$  is the mass transfer coefficient = 0.0003 m/s.

$$\alpha = \frac{1}{\frac{1}{\alpha_f} + \frac{\left(\frac{\delta Q_{SV}}{\delta Q_T}\right)}{\alpha_g}} \quad (2.3.17)$$

$$\frac{\delta Q_{SV}}{\delta Q_T} = \frac{\dot{m} x c_{pg} \delta T_G}{\dot{m} \Delta h_m} = \frac{x c_{pg} \Delta T}{\Delta h_m} \quad (2.3.18)$$

$$\alpha_m = \frac{1}{\frac{1}{\alpha_f} + \frac{\left(\frac{x c_{pg} \Delta T}{\Delta h_m}\right)}{\alpha_g}} \quad (2.3.19)$$

$$F_c = \frac{1}{\frac{\alpha_{fb,ia} \Delta T}{q_{nb}} (1 - \exp(-A))} \quad (2.3.20)$$

$$A = \frac{q_{nb}}{\rho_l \beta_l \Delta h_m} \quad (2.3.21)$$

$$\alpha_f = \alpha_{nb} F_c + \alpha_{cv} \quad (2.3.22)$$

## 2.4. Yun et al. (2002)

Yun et al. (2002) proposed a semi-empirical correlation to predict flow boiling HTC in microfin tubes for an experimental database of 749 data points. Yun et al. (2002) model does not consider the effect of helix angle in the model, hence the inclusion of variable helix angle data does not have any effect on the model predictions. This is a drawback in this model.

The two phase HTC is calculated using the single phase, smooth tube HTC term as base and modifying it using suitable terms to convert to two phase, microfin HTC correlation. The liquid HTC term is the Dittus-Boelter equation for heating. The  $HTC_{tp}$  term is a function of the boiling number and the Lockhart-Martinelli parameter.

$$HTC_{tp} = HTC_l \left[ C_1 Bo^{C_2} \left( \frac{P_{sat} D_i}{\sigma} \right)^{C_3} + C_4 \left( \frac{1}{X_{tt}} \right)^{C_5} \left( \frac{Gh}{\mu_l} \right)^{C_6} \right] Re_l^{C_7} Pr_l^{C_8} \left( \frac{\delta}{h} \right)^{C_9} \quad (2.4.1)$$

$$HTC_l = 0.023 Re_l^{0.8} Pr_l^{0.4} \frac{k_l}{d_i} \quad (2.4.2)$$

$$Re_l = G d_i / \mu_l \quad (2.4.3)$$

The boiling number (Bo) captures the effect of the nucleate boiling which is characterized by the presence of active nucleation sites and depends strongly on heat flux. The forced convection term is governed by the mass flow rate, vapor quality and the Lockhart-Martinelli parameter. Murata and Hashizume (1993) reported that the boiling number can be used for microfin tubes by modifying it using a term for the surface tension and turbulence. The enhancement term has the tendency to increase the HTC term due to the pronounced nucleate boiling at higher heat flux.

$$Bo = \frac{q}{h_{fg}G} \quad (2.4.4)$$

The single phase HTC is converted to two phase HTC by using the Lockhart-Martinelli parameter described in Yu et al. (1995).

$$X_{tt} = \left( \left( \frac{1-x}{x} \right)^{0.9} \left( \frac{\rho_g}{\rho_l} \right)^{0.5} \left( \frac{\mu_g}{\mu_l} \right)^{0.1} \right) \quad (2.4.5)$$

$\delta$  is the liquid film thickness for annular flows. It is assumed that in annular flow this liquid film thickness remains constant throughout the inner circumference of the microfin tube.

$$\delta = d_r \frac{1-\varepsilon}{4} \quad (2.4.6)$$

## 2.5. Chamra and Mago (2007)

Chamra and Mago (2007) used the Cavallini et al. (1999) model to predict experimental data for R22 and R134a. It was found that the R22 data was well predicted while the R134a data was not well predicted. Hence, Chamra and Mago (2007) proposed their own set of nine constants using the Cavallini et al. (1999) model. R410A was not considered in proposing the new constants. The equations of the Chamra and Mago (2007) model are the same as that in Cavallini et al. (1999)

Table 2.5.1. Table of constants as used in Chamra and Mago (2007)

	A	B	C	S	T	V	Z
Pure refrigerants	1.5160	1.1610	-1.7640	2.622	-0.2158	0.5927	0.0582
Mix refrigerants	0.7098	1.2040	3.3010	0.8317	0.1578	-1.0780	0.4217



## 2.6. Hamilton et al. (2008)

Hamilton et al. (2008) calculated the Nusselt number based on dimensionless parameters based on Cooper et al. (1984). The Nusselt number is based on the hydraulic diameter which is more representative of the actual area for the heat transfer as compared to root diameter. The six semi-empirical exponents were based on R134a for saturation temperatures of 0-30 °C. Cooper (1984) suggested that effect of nucleate boiling term can be captured as a ratio of reduced pressure and acentric factor  $-\log_{10}(P_r/P_c)$ . The M term is modified from the Cooper (1984) in order to make the equation dimensionless.

$$Nu = \frac{HTCd_h}{k_l} \quad (2.6.1)$$

$$Nu = 482.18Re_{lo}^{0.3}Pr^{C_1}\left(\frac{P_r}{P_c}\right)^{C_2}Bo^{C_3}\left(-\log_{10}\frac{P_r}{P_c}\right)^{C_4}M^{C_5}1.1^{C_6} \quad (2.6.2)$$

Constants  $C_1$  to  $C_5$  are based on vapor quality only.

$$C_1 = 0.51x \quad (2.6.3)$$

$$C_2 = 5.57x - 5.21x^2 \quad (2.6.4)$$

$$C_3 = 0.54 - 1.56x + 1.42x^2 \quad (2.6.5)$$

$$C_4 = -0.81 - 12.56x + 11x^2 \quad (2.6.6)$$

$$C_5 = -0.25 - 0.035x^2 \quad (2.6.7)$$

The constant  $C_6$  is specifically for refrigerant mixtures which considers the less volatile (LV) and more volatile (MV) components. This constant  $C_6$  becomes zero for pure refrigerants.

$$C_6 = \{(T_{LV} - T_{MV})[279.8(z_v - z_l) - 4298(T_d - T_b)/T_s]\}/T_s \quad (2.6.8)$$

## 2.7. Wu et al. (2013)

Wu et al. (2013) proposed an asymptotic model for R22 and R410A for 5 mm diameter tubes. Wu et al. (2013) also compared the data points to other existing models and showed that Thome et al. (1997) over-predicted the data while Yun et al. (2002) under-predicted the data. The Wu et al. (2013) model is based on Steiner and Taborek (1992) model for vertical tubes. The nucleate boiling term in Wu et al. (2013) correlation has terms similar to Yu et al. (1995) described in section 2.1.

$$HTC = ((HTC_{cv})^3 + (HTC_{nb})^3)^{1/3} \quad (2.7.1)$$

$$HTC_{nb} = S HTC_{pb} \quad (2.7.2)$$

$$S = 1/\xi (1 - \exp(-\xi)) \quad (2.7.3)$$

$$\xi = 1.96 \cdot 10^{-5} (\rho_l/\rho_v \cdot c_{pl}/h_{fg} \cdot T_{sat})^{1.25} (E_{rb} HTC_{cvi}) D_b/k_l \quad (2.7.4)$$

For heat fluxes less than the onset of nucleate boiling, the Wu et al. (2013) model sets the nucleate component of flow boiling to zero. This is because at very low fluxes the main mode of heat transfer is convection. As heat flux increases, nucleation begins to occur and then the nucleate boiling contributes to the heat transfer process.

if( $q > q_{onb}$ ) then

$$HTC_{pb} = 2.8 \cdot 207 k_l/D_b \left( \frac{(q-q_{onb}) D_b}{k_l T_{sat}} \right)^{0.745} (\rho_v/\rho_l)^{0.581} Pr_l^{0.533} \quad (2.7.5)$$

else

$$(HTC_{pb}) = 0 \quad (2.7.6)$$

$$A_c = 0.25 \pi d_i^2 - n_g h^2 \tan(\gamma/2) \quad (2.7.7)$$

A critical bubble radius ( $r_{crit}$ ) of  $0.38 \times 10^{-6}$  m. Constants  $C = 0.014$  and  $m = 0.68$  is given based on regression of the 503 data points.

$$q_{onb} = 2 \sigma T_{sat} \frac{HTC_{cvl}}{r_{crit} \rho_v h_{fg}} \quad (2.7.8)$$

$$D_b = 0.51 \left( \frac{2 \sigma}{g (\rho_l - \rho_v)} \right)^{0.5} \quad (2.7.9)$$

It is assumed that in annular flows the liquid is evenly distributed around the inner circumference of the tube. The  $\delta$  is the liquid film thickness which is used to calculate the convective boiling HTC based on Reynolds number. Enhancement factor  $E_{rb}$  is given by Ravigururajan and Bergels (1985).

$$HTC_{cv} = E_{rb} HTC_{cvl} \quad (2.7.10)$$

$$HTC_{cvl} = 0.014 Re_{\delta}^{0.68} Pr_l^{0.4} \frac{k_l}{\delta} \quad (2.7.11)$$

$$E_{rb} = \left( 1 + (2.64 Re_{\delta}^{0.036} Pr_l^{-0.024} (h/d_i)^{0.212} (p/d_i)^{-0.21} (\beta/90)^{0.29})^7 \right)^{1/7} \quad (2.7.12)$$

$$Re_{\delta} = 4 G (1 - x) \frac{\delta}{(1 - \varepsilon) \mu_l} \quad (2.7.13)$$

$$\delta = \sqrt{A_c / \pi} \left( 1 - \sqrt{\varepsilon} \right) \quad (2.7.14)$$

Pitch and void fraction are the same as explained in Thome et al. (1997).

$$p = \pi d_i / n_g \quad (2.7.15)$$

$$\varepsilon = \left( \frac{x}{\rho_v} \right) \left( (1 + 0.12(1 - x)) \left( \frac{x}{\rho_v} + \frac{1-x}{\rho_l} \right) + 1.18(1 - x) \frac{(g \sigma (\rho_l - \rho_v))^{0.25}}{G \rho_l^{0.5}} \right)^{-1} \quad (2.7.16)$$

### 3. Experimental flow boiling HTC data

The experimental database consists of 2201 data points. Tables 3.1, 3.2, and 3.3 provide details of the refrigerant, operating and geometric parameters of the database under consideration. In the tables the \* mark indicates that the value is not given in the reference publication and hence is assumed. These experimental data points were collected from their respective publications using the DigitizeIt software (Copyright 2001-2015 I. Bormann). This software was used so that the experimental data points can be collected with maximum accuracy and avoid errors involved in reading data manually.

Table 3.1. Experimental database summary – Refrigerant properties and no. of data points

Reference	Runs	Refrigerant	Tsat (°C)	Comments
Akhavan-Behabadi et al. (2011)	20	R134a	-14.5	4 mass fluxes and inclined tubes.
Baba et al. (2012)	148	R32, R1234ZE	10	Study of R32-R1234ZE: pure and mixtures. Only pure refrigerant considered here.
Cho and Kim (2007)	200	CO <sub>2</sub>	10	2 tubes tested for 3 values of mass and heat fluxes each.
Cho et al. (2009)	20	CO <sub>2</sub>	-5	Vapor quality varied for two values of heat and mass flux
Dang et al. (2010)	71	CO <sub>2</sub>	15	2 mm diameter tubes for 2 values of mass and heat fluxes each.
Del Col et al. (2007)	24	R22	22	Helical tubes tested for 2 mass and heat fluxes each.
Diani et al. (2014)	164	R1234 ZE	30	R1234ZE tested for 3.64 mm tube for 2 values of mass fluxes and 3 values of heat fluxes.
Eckels et al. (1994)	4	R134a	1	Lubricant mixtures studied. (Only pure refrigerant considered in this study.)
Filho and Barbeiri (2010)	117	R134a	5	2 tubes of identical dimensions with different surface roughness tested.
Filho and Jabardo (2006)	39	R134a	5	Comparison between herringbone and microfin tubes.
Gao and Honda (2006)	111	CO <sub>2</sub>	10	CO <sub>2</sub> -oil mixtures for small diameter tubes.
Hu et al. (2008)	18	R410A	5	R410A-oil mixtures studied.
Jiang et al. (2016)	60	R410A, R134a, R22, R407C	5	Quality, mass and heat flux was varied for 4 refrigerants flowing

				through 8.92 mm diameter tubes.
Kabelac and Buhr (2000)	81	Ammonia	-20	Ammonia was tested in 11.13 mm tubes for 2 heat fluxes and 3 mass fluxes.
Kim and Shin (2005)	57	R410A, R22	15	7 tubes tested for constant x and varying G and q.
Kim et al. (2007)	83	CO <sub>2</sub>	-5 - 0	Flow and heat transfer studied in vertical and horizontal tubes.
Kimura and Ito (1981)	21	R12	-.831- 6	Relatively low flow rates.
Kondou et al. (2013)	34	R32, R1234ze	10	Study of R32-R1234ZE. (Pure R32, 20% R32, 50% R32, 80% R32 and pure R1234ZE). Only pure refrigerant considered here.
Kuo and Wang (1996)	67	R22, R407C	1.66 - 6.04	2 refrigerants studied for 3 heat fluxes.
Mancin et al. (2014)	63	R134a	30	R134a in 3.4 mm diameter tube. Tested for 2 mass fluxes and 3 heat fluxes.
Padovan et al. (2011)	239	R134a, R410A	29.7- 39.9	2 refrigerants for high Tsat with changing heat and mass fluxes.
Rollmann et al. (2011)	70	R407C	10	For quality and mass flux fixed, heat flux was varied
Rollmann et al. (2016)	41	R407C	-10	Heat flux was varied from 1- 20 kW/m <sup>2</sup> for mass flux of 300 kg/m <sup>2</sup> -s
Schael and Kind (2005)	24	CO <sub>2</sub>	5	3 mass fluxes with varying quality from almost 10- 95%
Spindler et al. (2009)	133	R134a, R404A	-20	2 refrigerants studied for low mass and heat fluxes.
Spindler, Muller-Steinhagen (2009)	206	R134a	-20	R134a in 8.92 mm tubes for varying mass and heat fluxes keeping vapor quality constant.
Wongsa-ngam et al. (2004)	39	R134a	15	Medium to high mass fluxes.
Wu et al. (2013)	47	R22, R410A	6	5 different tubes with different number of fins and helix angles are tested.

Table 3.2. Experimental database summary – Operating conditions

Reference	G (kg/m <sup>2</sup> - s)	x (%)	Local or avg. HTC	q (W/m <sup>2</sup> )
Akhavan-Behabadi et al. (2011)	53-136	20-95	Local	2100-5300
Baba et al. (2012)	150-400	10-90	Local	5000-15000
Cho and Kim (2007)	212-656	10-95	Average	6000-20000
Cho et al. (2009)	318,656	10-85	Local	15000,30000
Dang et al. (2010)	360-720	10-95	Local	9000-18000
Del Col et al. (2007)	205-225	10-80	Local	5500-9200
Diani et al. (2014)	375-940	20-97	Local	10000-50000
Eckels et al. (1994)	85-367	50-85	Average	8000-34000
Filho and Barbeiri (2010)	100-500	5-95	Average	5000
Filho and Jabardo (2006)	100-500	10-90	Average	5000
Gao and Honda (2006)	190-770	10-95	Local	10000-30000
Hu et al. (2008)	200-400	25-90	Local	7560-15120
Jiang et al. (2016)	250-500	10-80	Average	5000-20000
Kabelac and Buhr (2000)	50-150	1-60	Local	40000,50000
Kim and Shin (2005)	210*	10-85	Local	11000
Kim et al. (2007)	212-424	4-80	Average	15000-45000
Kimura and Ito (1981)	30-160	55	Local	18700-44900
Kondou et al. (2013)	191-382	20-90	Local	10000
Kuo and Wang (1996)	100-300	15-90	Average	6000-14000
Mancin et al. (2014)	190-755	20-99	Mostly local	10000-50000
Padovan et al. (2011)	80-600	20-90	Local	14700-44200
Rollmann et al. (2011)	25-300	10-80	Average	800-19600
Rollmann et al. (2016)	300	10-85	Local	1000-20000
Schael and Kind (2005)	75-500	10-90	Local	4100-59900
Spindler et al. (2009)	24-151	10-70	Average	10000-15000
Spindler,Muller-Steinhagen (2009)	25-150	10-70	Average	1000-15000
Wongsa-ngam et al. (2004)	400-800	25-80	Average	10000
Wu et al. (2013)	96-583	10-80	Average	9978-32031



Table 3.3. Experimental database summary – Geometric conditions

Reference	Root diameter (mm)	Fin height (mm)	Apex angle (deg.)	Helix angle (deg.)	No. of fins
Akhavan-Behabadi et al. (2011)	8.92	0.25	25	15	55
Baba et al. (2012)	5.37	0.256	50	18	58
Cho and Kim (2007)	4.4, 8.92	0.12, 0.15	50	18	60
Cho et al. (2009)	4.5	0.15	50	18	60
Dang et al. (2010)	1.996	0.117	34.8	6.3	40
Del Col et al. (2007)	14.85	0.36	41.6	21.5	73
Diani et al. (2014)	3.64	0.12	43	18	40
Eckels et al. (1994)	8.52	0.2	50	17	60
Filho and Barbeiri (2010)	8.92	0.2	50*	18	60
Filho and Jabardo (2006)	8.92	0.2	33	18	82
Gao and Honda (2006)	3.04	0.11	40.5	18	40
Hu et al. (2008)	6.5	0.18	40	18	50
Jiang et al. (2016)	8.96	0.14	33	18	60
Kabelac and Buhr (2000)	11.13	0.63	0	25	21
Kim and Shin (2005)	8.8, 8.82	0.12, 0.195, 0.25	40, 50	25, 30	54
Kim et al. (2007)	4.5	0.15	50*	18	60
Kimura and Ito (1981)	4.75	0.1	136	4	31
Kondou et al. (2013)	5.45	0.225	50	20.1	48
Kuo and Wang (1996)	8.92	0.2	50*	18	60
Mancin et al. (2014)	3.64	0.12	50*	18	40
Padovan et al. (2011)	8.15	0.23	43	13	60
Rollmann et al. (2011)	8.95	0.24	25	15	55
Rollmann et al. (2016)	8.95	0.24	25	15	55
Schael and Kind (2005)	8.62	0.25	30	18	60
Spindler et al. (2009)	8.92	0.24	20	15	55
Spindler, Muller-Steinhagen (2009)	8.95	0.24	50*	15	55
Wongsa-ngam et al. (2004)	8.92	0.2	50*	18	60
Wu et al. (2013)	4.54, 4.6	0.1-0.15	35-58	18-25	35-58

Mathematically, for higher MAD and SD values the X30% value should be low and vice versa. A sample plot is shown in Figure 3.1 which shows the variation of MAD and SD with X30%. For this sample plot, Cavallini et al. (1999) is compared with some of the experimental data from the database. These plots can also be extended for all the experimental data for different correlations. For the purpose of clarity and simplicity, only one correlation has been plotted here against few experimental references. From Figure 3.1 it can be seen that, in general, MAD and SD increase simultaneously while X30% decreases. However, there can be few exceptions. Merchant and Mehendale (2015) have reported that different correlations predict the same experimental points very differently. It is shown that none of the correlations are sufficient to predict the experimental data points accurately. The purpose of the current research is to provide a model that is of use to the practicing engineer to predict flow boiling HTC's over a wide range of geometric and operating parameters.

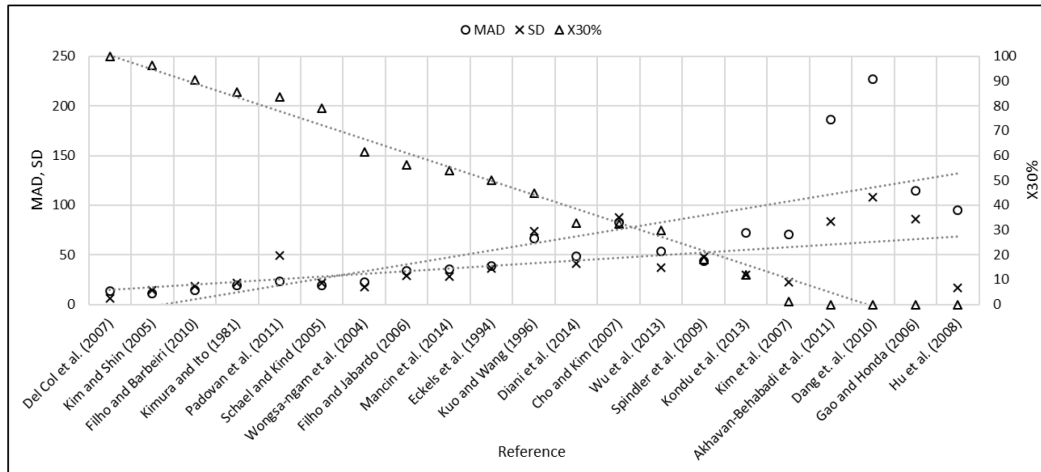


Figure 3.1. Graph showing the variation of MAD and SD against X30% for experimental references in published literature

#### 4. New model to predict flow boiling HTC in microfin tubes

The linearized model proposed consists of dimensionless or pi terms. These dimensionless terms are coined carefully to avoid repetition of parameters. These dimensionless terms capture the effects of geometry, operating parameters and refrigerant properties. Also, repetition of variables is avoided. For example, as the convective boiling term (Co) consist of the density ratio, this density ratio does not repeat in equation (4.1). Equation (4.1) shows the main mathematical form. Equations (4.2) - (4.7) define the dimensionless terms used in equation (4.1).

From the study of existing correlations, it is seen that the HTC models are generally proposed as an additive and asymptotic combination of the nucleate and convective boiling terms. For the new model, the smooth tube Nusselt number is modified using terms to capture the effect of two phase flows and microfins. The smooth tube Nusselt number is given by the Dittus- Boelter correlation.

$$\frac{HTC d_h}{k_l} = C_0 Nu_{smooth}^{C_1} Bo^{C_2} Co^{C_3} Rx^{C_4} Fr^{C_5} \left(\frac{\mu_l}{\mu_g}\right)^{C_6} \left(\frac{q^2}{h_{fg} \times P_{sat}^2}\right)^{C_7} \quad (4.1)$$

$$Nu_{smooth} = 0.023 \left(\frac{G d_i}{\mu_l}\right)^{0.8} Pr_l^{0.4} \quad (4.2)$$

$$Pr_l = \frac{\mu_l \cdot Cp_l}{k_l} \quad (4.3)$$

$$Bo = \frac{g \rho_l h \pi d_i}{8 \sigma n_g} \quad (4.4)$$

$$Co = \left(\frac{1-x}{x}\right)^{0.8} \left(\frac{\rho_l}{\rho_g}\right)^{-0.5} \quad (4.5)$$

$$Rx = \frac{\frac{2hn_g(1-\sin(\gamma/2))}{\pi d_i \cos(\gamma/2)} + 1}{\cos \beta} \quad (4.6)$$

$$Fr = \frac{\left(\frac{G}{\rho g}\right)^2}{g d_i} \quad (4.7)$$

The convective HTC is captured by the Froude number (Fr), the ratio of inertia force to gravity force, which is dependent on the mass flux and convective boiling term (Co) which depends on vapor quality and is the two phase multiplier. The capillary effect is captured by the Bond number (Bo) which is the ratio of gravity to surface tension. The presence of microfins causes the liquid to be drawn to the upper side of the tube, thus causing the wetting of the entire surface at lower mass fluxes which is the combined effect of the swirl and the surface tension. Rx is the ratio between the enhanced area for heat transfer for the axial microfin tubes to the smooth tube area. It is a term that can be derived geometrically per unit tube length as follows.

$$Rx = \frac{A}{A_{smooth}} \quad (4.8)$$

$$A_{smooth} = \pi d_i \quad (4.9)$$

$$A = \frac{\left(\frac{h}{\cos(\frac{\gamma}{2})} + \frac{h}{\cos(\frac{\gamma}{2})} + \frac{\pi d_i}{n_g} - 2h \tan(\frac{\gamma}{2})\right) n_g}{\cos \beta} \quad (4.10)$$

$$Rx = \frac{\left(\frac{2h}{\cos(\frac{\gamma}{2})} + \frac{\pi d_i}{n_g} - 2h \tan(\frac{\gamma}{2})\right) n_g}{\pi d_i \cos \beta} \quad (4.11)$$

$$Rx = \frac{\frac{2h n_g}{\cos(\frac{\gamma}{2})} (1 - \sin(\frac{\gamma}{2})) + \pi d_i}{\pi d_i \cos \beta} \quad (4.12)$$

$$Rx = \frac{\frac{2h n_g}{\pi d_i \cos(\frac{\gamma}{2})} (1 - \sin(\frac{\gamma}{2})) + 1}{\cos \beta} \quad (4.13)$$

The nucleate boiling has a strong dependence on heat flux. If the heat flux is less than the heat flux for onset of nucleate boiling, then the nucleate boiling component is negligible.

This term is captured by  $\frac{q^2}{h_{fg} P_{sat}^2}$ . This is a term that is derived by using the Buckingham pi theorem as follows.

$$[q^a] [h_{fg}^b] [P_{sat}^c] = M^0 L^0 T^0 \quad (4.14)$$

The variables a, b, c are random exponents whose numerical values need to be determined.

$$[M^a T^{-3a}] [L^{2b} T^{-2b}] [M^c L^{-c} T^{-2c}] = M^0 L^0 T^0 \quad (4.15)$$

$$M^{a+c} L^{2b-c} T^{-3a-2b-2c} = M^0 L^0 T^0 \quad (4.16)$$

Equating the exponents on both sides of the equation we get,

$$a + c = 0 \quad (4.17)$$

$$2b - c = 0 \quad (4.18)$$

$$-c - 2c + 3c = 0 \quad (4.19)$$

On solving these equations simultaneously, we see that any numerical value can satisfy these equations without affecting the result. Hence the value selected was a=2, h<sub>fg</sub>= -1,

P<sub>sat</sub>= -2. This is how the term  $\frac{q^2}{h_{fg} P_{sat}^2}$  has been derived.

The X30% values show that any given model does not predict flow boiling HTC's well for the full dataset consisting of 2201 points of individual datasets when divided into refrigerant categories- halogenated refrigerant, CO<sub>2</sub> and NH<sub>3</sub>. The reason to have this division of the experimental data is based on the fact that properties for each of these classes of refrigerants is distantly disparate. The graphs given below show the properties on the Y axis and saturation temperature on the X axis. From figure 4.1 (density ratio) it is clear that NH<sub>3</sub> has a very high value of  $\rho_l/\rho_g$  which is almost four times that of halogenated refrigerants while CO<sub>2</sub> lies on a very low band in the graph. Similar conclusions can be drawn from Figures 4.2-4.5. By looking at these property plots it is clear that all the refrigerants cannot be classified in the same manner. There has to be a distinguishing parameter in the model proposed for a wide applicability. For this purpose, different set of constants C<sub>0</sub> to C<sub>7</sub> are proposed to distinguish the model for different refrigerant categories. The constants C<sub>0</sub> to C<sub>7</sub> are defined in Table 4.1. These constants were obtained by linearized least squares minimization approach in R software (<https://www.r-project.org/>). For regression, the logarithm was taken on both sides of equation (4.1) to give the following equation.

$$\ln\left(\frac{HTC}{k_l} \frac{d_h}{k_l}\right) = \ln(C_0) + C_1 \ln(Nu_{smooth}) + C_2 \ln(Bo) + C_3 \ln(Co) + C_4 \ln(Rx) + C_5 \ln(Fr) + C_6 \ln\left(\frac{\mu_l}{\mu_g}\right) + C_7 \ln\left(\frac{q^2}{\rho_{fg} P_{sat}^2}\right) \quad (4.20)$$

This is now an equation which can be solved by the linearized least squares technique and hence the title of the model is given as 'linearized' model. This least squares method was run in R software. A sample output of R software is given below.

Coefficients:

	Estimate	Std. Error	t value	Pr(> t )
(Intercept)	15.19394	0.79235	19.176	< 2e-16 ***
ln(NU <sub>smooth</sub> )	-0.35864	0.06347	-5.651	1.83e-08 ***
lnBo	0.24059	0.02973	8.091	1.03e-15 ***
lnCo	-0.15948	0.02653	-6.012	2.18e-09 ***
lnRx	-1.09601	0.12900	-8.496	< 2e-16 ***
lnFr	0.18686	0.02792	6.692	2.86e-11 ***
ln( $\mu_1/\mu_g$ )	-0.57383	0.03947	-14.538	< 2e-16 ***
ln( $q^2/h_{fg}P_{sat}^2$ )	-0.85737	0.05784	-14.824	< 2e-16 ***

The first column, “estimate” is for point estimation. These values are the estimated coefficients.

Due to the randomness in data, these point estimates can (almost) never hit the true parameter (true coefficient values). For this reason, in statistics we talk about confidence interval or hypothesis testing rather than just relying on a point estimate.

‘Std.Error’ columns report the standard errors of these point estimates. 95% Confidence interval can be constructed using the point estimates and the standard errors (more specifically, point estimate  $\pm 2$ \*standard error is your 95% confidence interval of the true parameter).

‘t value’ column is for hypothesis testing. More specifically, t value = estimate/Std.Error.

The most important column is Pr(>|t|). This reports the p-value.

The default R output conducts hypothesis testing to test-

Null hypothesis: the true parameter (coefficient) is zero vs

Alternative hypothesis: The true parameter is not zero.

To argue that  $\ln(Nu_{smooth})$  does have a linear effect on  $\ln(Nu_{expt})$ , you want to provide strong enough evidence to support the alternative hypothesis, or in other words, to provide strong enough evidence against the null hypothesis. Thus, null hypothesis is rejected if the probability of observing data is very small, assuming that the null hypothesis is true. This probability is called p-value. If the p-value is smaller than the significance level (a preset value - conventionally 0.05), then the null hypothesis is rejected. The significance level is the amount of risk taking in falsely and rejecting the null hypothesis. By taking it to be 0.05, this means only 5% chance to make mistake is allowed (=reject the null hypothesis when it is true). This serves as a strong evidence against the null hypothesis.

For the given results, all the p-values are much smaller than 0.05. These are almost zeros. This means all the explanatory variables (the variables on the right hand side) have very strong linear effect on the response variable (the variable on the left hand side of the equation,  $\ln(Nu_{expt})$ ). We say, for example,  $\ln(Nu_{smooth})$  is significant. This means all the variables in the model must be kept. For the purpose of estimating the coefficients, the point estimates can be used.



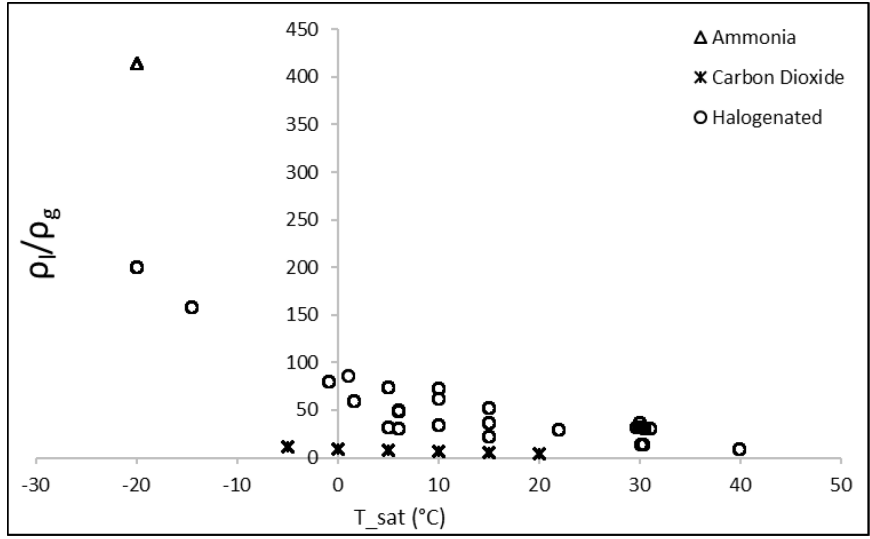


Figure 4.1. Property plot of density ratio vs. saturation temperature for different refrigerants.

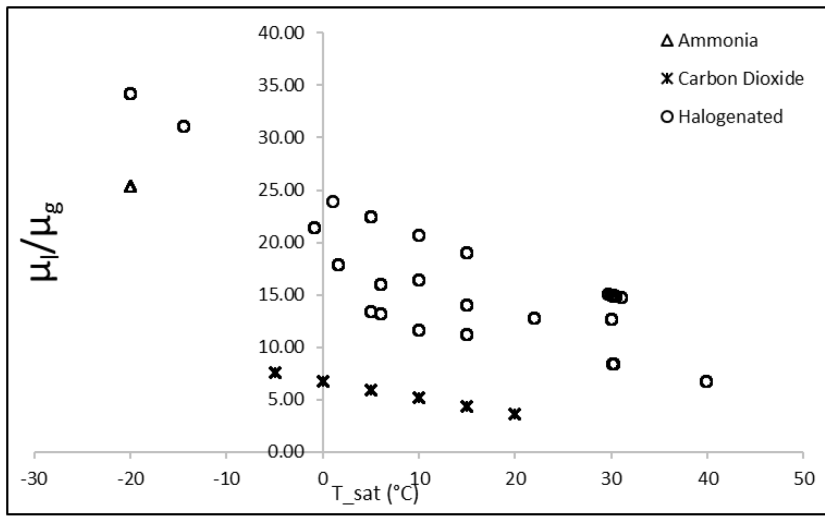


Figure 4.2. Property plot of viscosity ratio vs. saturation temperature for different refrigerants.

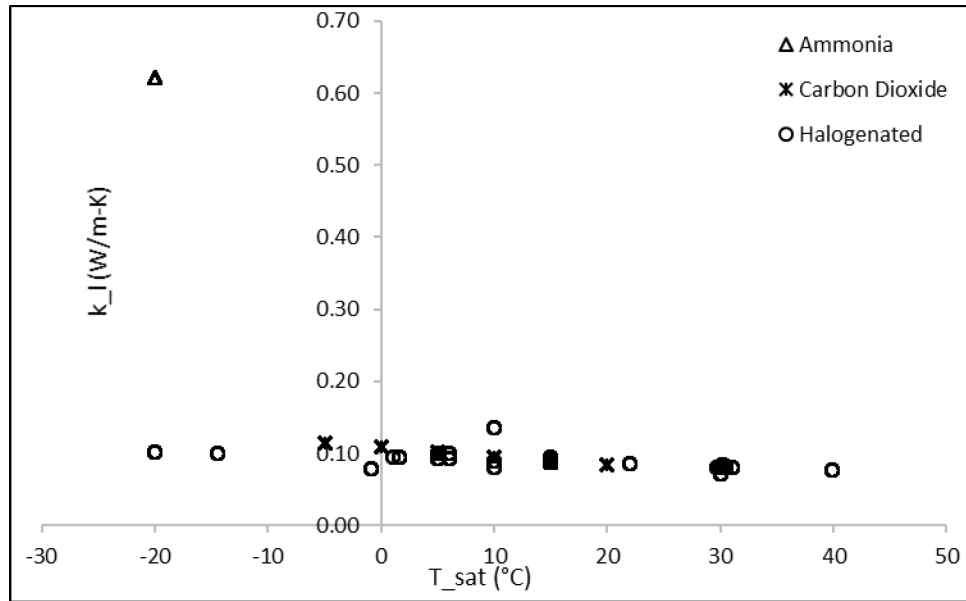


Figure 4.3. Property plot of thermal conductivity vs. saturation temperature for different refrigerants.

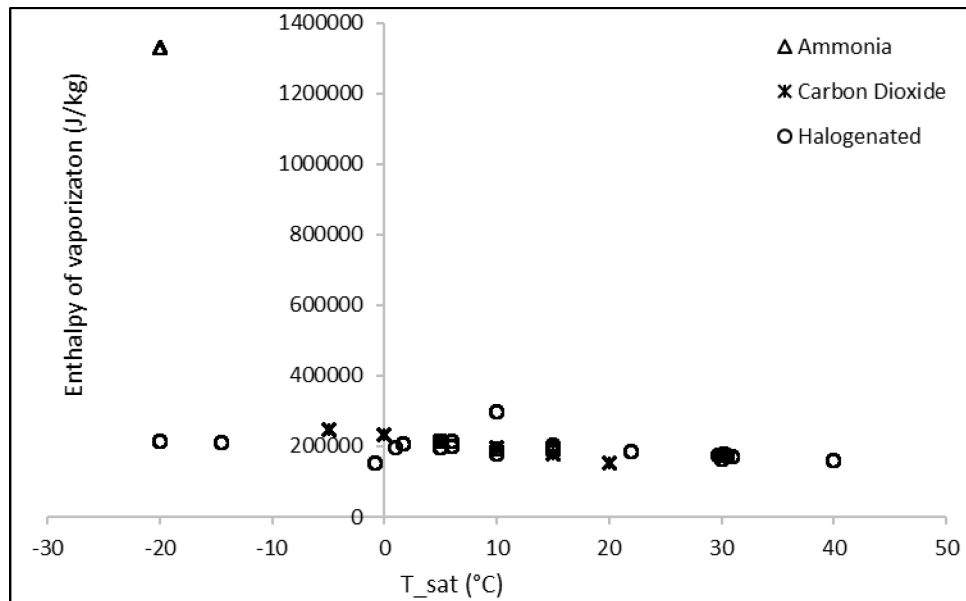


Figure 4.4. Property plot of enthalpy of vaporization vs. saturation temperature for different refrigerants.

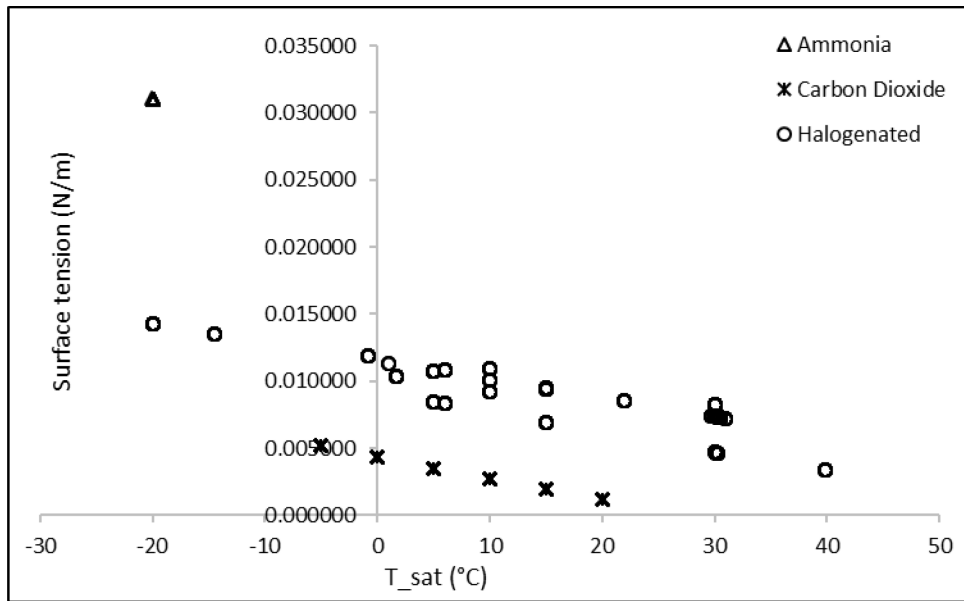


Figure 4.5. Property plot of surface tension vs. saturation temperature for different refrigerants.

From the Figures 4.1-4.5, it is seen that the halogenated refrigerants can be seen as a single band on the property plots. However, if the constants for all halogenated refrigerants were clubbed into a single set of values for  $C_0$  to  $C_7$  then the model did not predict flow boiling HTC's well across the range of halogenated refrigerants. Also, it is known the refrigerant mixtures do not have the same characteristics as pure refrigerants (Jung and Radermacher (1990)). The different components of a refrigerant mixture boil at specific saturation temperatures. Hence, refrigerant mixtures show a temperature glide instead of a single boiling point. Hence, the division of constants also needs to be made for pure and mixed refrigerants within halogenated refrigerants. Refrigerant mixtures from the database

include R410A, R407C, R1234ZE(e). For example, R410A is a near-azeotropic mixture of R-32 (50%) and R-125 (50%) while R407C consists of R-32 (23%), R-134a (52%) and R-125 (25%).

In addition, it was observed that the linearized model with constants for only pure and mixed refrigerant divide did not perform well for low heat flux ( $<5000 \text{ W/m}^2$ ) applications. Hence for low heat flux applications a separate set of constants has been recommended. The Table 4.1 shows the set of constants to be applied to the linearized model as described in equation (4.1).

Table 4.1. Constants to be used in the linearized model for different categories

Category	C <sub>0</sub>	C <sub>1</sub>	C <sub>2</sub>	C <sub>3</sub>	C <sub>4</sub>	C <sub>5</sub>	C <sub>6</sub>	C <sub>7</sub>
NH <sub>3</sub>	175.483	0.72208	0.04853	-0.13723	-0.36891	-0.21916	0.87680	0.11329
CO <sub>2</sub>	211362.511	0.34549	0.59370	0.08940	-1.25179	-0.04198	0.30594	0.20388
Halogenated (pure) ( $q > 5000 \text{ W/m}^2$ )	30223.045	0.11531	0.81214	-0.12773	-1.21380	0.06382	0.07677	0.05367
Halogenated (mix) ( $q > 5000 \text{ W/m}^2$ )	65.272	1.09355	-0.16319	-0.07956	0.91003	-0.24131	0.37526	0.15324
Halogenated ( $q < 5000 \text{ W/m}^2$ )	6676.372	-1.38227	-1.14169	-0.13940	-3.14520	0.69652	-2.02970	-0.01360

## 5. Results and discussion

### 5.1. Global evaluation of the new model

The MD, MAD, SD and X30% is given in Table 5.1.1.-5.1.4. Comparing these values, it can be seen that the linearized model performs better statistically for all datasets.

Table 5.1.1. MD comparison

MD	New model	Cavallini et al. (1999)	Wu et al. (2013)	Thome et al. (1997)	Hamilton et al. (2008)	Chamra and Mago (2007)	Yu et al. (1995)	Yun et al. (2002)
All data	3.9	47.8	30.4	86.2	-34.0	90.0	1.9	-43.2
Carbon dioxide	4.0	105.3	54.5	35.5	-70.4	174.8	53.7	-53.9
Ammonia	29.1	52.3	33.3	231.4	-61.1	47.8	-64.8	-78.0
Halogenated (all)	2.6	29.4	22.6	94.9	-21.1	65.4	-11.2	-38.1
Pure Halogenated	2.5	33.0	18.7	96.4	-23.0	69.3	-12.5	-39.0
Mix Halogenated	2.7	25.8	26.5	93.3	-19.3	61.4	-9.8	-37.3

Table 5.1.2. MAD comparison

MAD	New model	Cavallini et al. (1999)	Wu et al. (2013)	Thome et al. (1997)	Hamilton et al. (2008)	Chamra and Mago (2007)	Yu et al. (1995)	Yun et al. (2002)
All data	23.6	64.6	57.7	95.7	48.2	105.0	50.2	65.8
Carbon dioxide	22.6	108.4	58.0	51.6	71.3	176.7	57.4	66.2
Ammonia	30.1	52.3	39.0	231.4	61.9	49.3	64.8	78.0
Halogenated (all)	23.5	51.4	58.6	102.8	40.2	85.2	47.2	65.0
Pure Halogenated	20.6	58.9	55.1	111.0	36.5	90.2	40.3	62.4
Mix Halogenated	26.4	43.9	62.1	94.6	43.9	80.3	54.0	67.6

Table 5.1.3. SD comparison

SD	New model	Cavallini et al. (1999)	Wu et al. (2013)	Thome et al. (1997)	Hamilton et al. (2008)	Chamra and Mago (2007)	Yu et al. (1995)	Yun et al. (2002)
All data	38.7	86.7	91.7	144.0	47.4	146.0	69.2	80.8
Carbon dioxide	32.0	102.1	74.2	87.6	24.4	205.2	70.8	50.3
Ammonia	23.7	31.5	36.4	62.1	19.6	145.4	10.4	12.0
Halogenated (all)	40.8	74.5	97.2	154.2	47.4	108.7	61.0	89.4
Pure Halogenated	38.3	76.8	95.3	157.9	45.3	116.5	52.9	85.9
Mix Halogenated	43.3	72.2	99.0	150.5	49.5	100.9	69.0	92.9

Table 5.1.4. X30% comparison

X30%	New model	Cavallini et al. (1999)	Wu et al. (2013)	Thome et al. (1997)	Hamilton et al. (2008)	Chamra and Mago (2007)	Yu et al. (1995)	Yun et al. (2002)
All data	76.5	36.8	38.3	37.6	33.9	28.3	33.5	12.7
Carbon dioxide	77.4	17.1	43.2	56.2	7.9	16.1	39.3	10.8
Ammonia	61.7	22.2	49.4	0.0	7.4	57.9	1.2	2.5
Halogenated(all)	77.0	43.8	36.1	33.6	43.5	30.1	33.3	13.8
Pure Halogenated	73.6	48.6	34.7	43.1	32.1	38.0	30.1	11.4
Mix Halogenated	79.8	35.4	38.7	17.2	60.1	16.4	38.8	17.7

Scatter plots are shown in Figure 5.1.1. From visual inspection of Figure 5.1.1., it can be seen that the linearized model predicts data well within the  $\pm 30\%$  lines and that the linearized model is superior to the existing models.

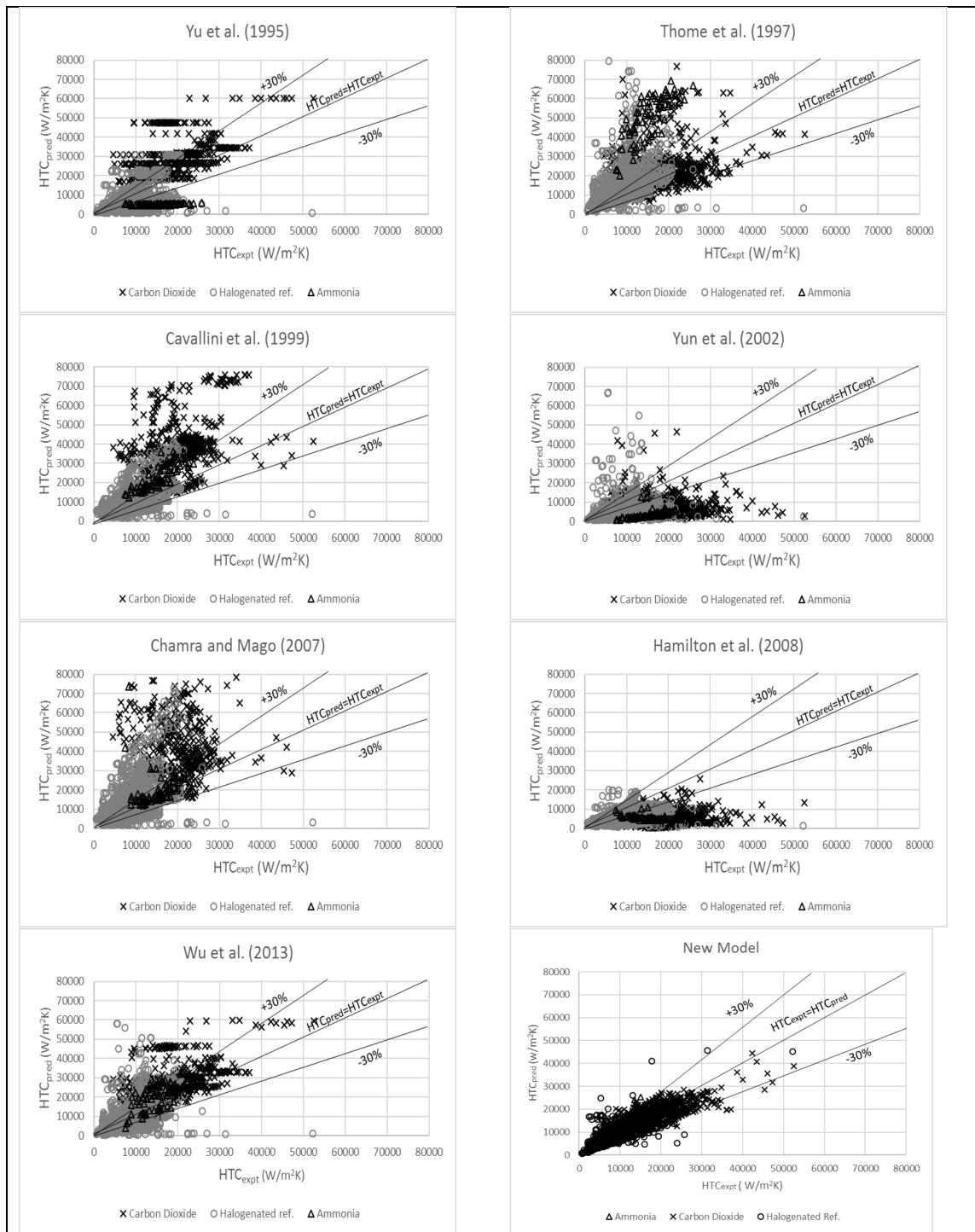


Figure 5.1. 1. Scatter plots of the predicted HTC of models vs. experimental HTC.

The constants given in table 4.1. were selected after careful deliberation. The full dataset was sorted in different ways – based on diameter, mass flux, heat flux and refrigerant. The full dataset of 2201 points was divided into the sections as given in table 5.1.5. The constants  $C_0$  to  $C_7$  for each section was derived by linearized regression using R software. In order to assess the sensitivity of the constants to the diameter, heat flux, mass flux and refrigerants, the correct way to would be check the partial derivatives of the equation (4.1). However, due to the complex mathematical formulation, a grid sensitivity study was carried out. The experimental database of 2201 points was sorted according to diameter, heat flux, mass flux and refrigerants. Further, subdivisions were made as shown in table 5.1.5. For example, the case “5 sort (pure mix  $q < 5000$ )” the dataset was first divided based on refrigerants -  $CO_2$ ,  $NH_3$ , pure halogenated refrigerants and mixed halogenated refrigerants. Constants  $C_0$  to  $C_7$  were derived for this dataset. It was observed that the constants did not predict data well for the category halogenated refrigerants ( $q < 5000$   $W/m^2$ ). Hence this category was separated and different set of constants  $C_0$  to  $C_7$  were derived for this category. Similar exercise was carried out for the remaining datasets which are reported in table 5.1.5. The X30% of these datasets were calculated and plotted as shown in Figure 5.1.2. From this figure, it is clear that the linearized model for all datasets perform better than the existing correlations. However, for the category “5 sort (pure mix  $q < 5000$ )” performs the best compared to all other linearized models. Hence the coefficients  $C_0$  to  $C_7$  that were derived from this category are selected to be used and reported in this thesis.



Table 5.1.5. Dataset divisions for deriving constants to select the best model to predict flow boiling HTC for microfin tubes.

<b>Terminology</b>	<b>Dataset divisions</b>
5 sort (pure mix $q < 5000$ )	<ul style="list-style-type: none"> <li>• CO<sub>2</sub></li> <li>• NH<sub>3</sub></li> <li>• Pure halogenated refrigerants</li> <li>• Mixed halogenated refrigerants</li> <li>• Halogenated refrigerants (<math>q &lt; 5000 \text{ W/m}^2</math>)</li> </ul>
5 sort (q based)	<ul style="list-style-type: none"> <li>• CO<sub>2</sub></li> <li>• NH<sub>3</sub></li> <li>• Halogenated refrigerants (<math>q \leq 5000 \text{ W/m}^2</math>)</li> <li>• Halogenated refrigerants (<math>5000 &lt; q \leq 10000 \text{ W/m}^2</math>)</li> <li>• Halogenated refrigerants (<math>q &gt; 10000 \text{ W/m}^2</math>)</li> </ul>
d sort	<ul style="list-style-type: none"> <li>• CO<sub>2</sub></li> <li>• NH<sub>3</sub></li> <li>• Halogenated refrigerants (<math>d \leq 5 \text{ mm}</math>)</li> <li>• Halogenated refrigerants (<math>d &gt; 5 \text{ mm}</math>)</li> </ul>
T <sub>sat</sub> 5 sort	<ul style="list-style-type: none"> <li>• CO<sub>2</sub></li> <li>• NH<sub>3</sub></li> <li>• Halogenated refrigerants (<math>T_{\text{sat}} \leq 0^\circ\text{C}</math>)</li> <li>• Halogenated refrigerants (<math>0 &lt; T_{\text{sat}} \leq 5^\circ\text{C}</math>)</li> <li>• Halogenated refrigerants (<math>T_{\text{sat}} &gt; 5^\circ\text{C}</math>)</li> </ul>
T <sub>sat</sub> sort	<ul style="list-style-type: none"> <li>• CO<sub>2</sub></li> <li>• NH<sub>3</sub></li> <li>• Halogenated refrigerants (<math>T_{\text{sat}} \leq 0^\circ\text{C}</math>)</li> <li>• Halogenated refrigerants (<math>T_{\text{sat}} &gt; 0^\circ\text{C}</math>)</li> </ul>
G sort	<ul style="list-style-type: none"> <li>• CO<sub>2</sub></li> <li>• NH<sub>3</sub></li> <li>• Halogenated refrigerants (<math>G \leq 300 \text{ kg/m}^2\text{s}</math>)</li> <li>• Halogenated refrigerants (<math>G &gt; 300 \text{ kg/m}^2\text{s}</math>)</li> </ul>
q sort	<ul style="list-style-type: none"> <li>• CO<sub>2</sub></li> <li>• NH<sub>3</sub></li> <li>• Halogenated refrigerants (<math>q \leq 5000 \text{ W/m}^2</math>)</li> <li>• Halogenated refrigerants (<math>q &gt; 5000 \text{ W/m}^2</math>)</li> </ul>

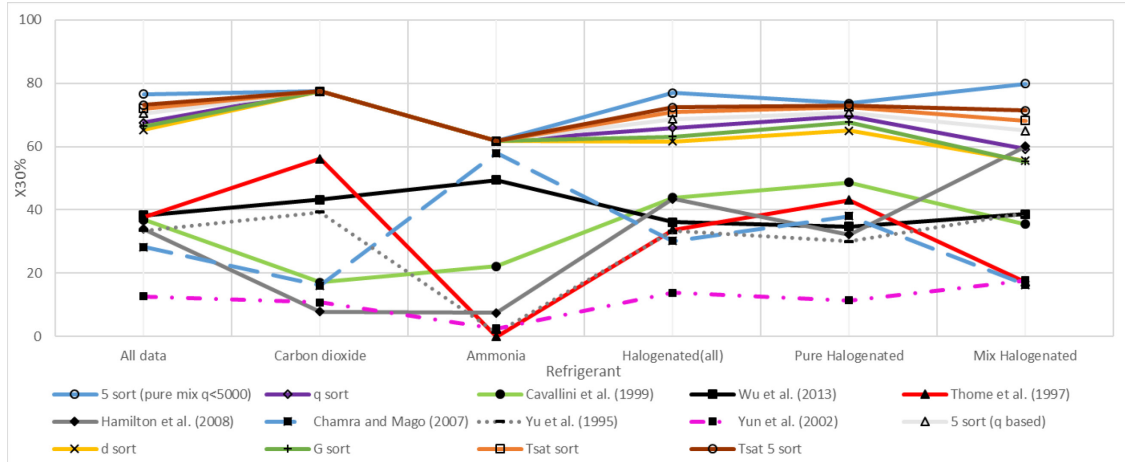


Figure 5.1.2. X30% values for each dataset division for deriving constants to select the best model to predict flow boiling HTC for microfin tubes.

## 5.2. Application-specific evaluation of the new model

Existing models report MD, MAD and SD to show the accuracy of the models. Even X30% is a statistical quantity that can be used to give the numerical accuracy of the correlations. However, it is known that even if the models have high values of X30% they do not represent the applicability of the model to a particular set of data. The engineers in the industry require application-specific guidelines as to which correlation can be used for different data sets. Hence it is important to perform a trend study where the models are tested against specific sets of experimental data to see how a correlation performs in those cases. For this thesis, a comprehensive dataset has been used. 45 trends were studied, which are subsets of the experimental database given in section 3. Figures 5.2.1 – 5.2.7 show the comparison of specific experimental data with respect to the new and the best among existing models. Similar to these figures, many other datasets for different experimental data have been plotted. For clarity, out of the 45 cases studied, seven representative figures are reported in the current work. The remaining cases studied are shown in the appendix.

For CO<sub>2</sub>, the following 11 cases were studied. As seen in table 5.2.1, these 11 cases cover a wide range of diameters, heat and mass fluxes for CO<sub>2</sub>. Out of these 11 cases studied, in 9 cases (case numbers- 1, 2, 4, 5, 6, 8, 9, 10, 11 in table 5.2.1) the new model is superior to the all the existing models. Hence, if an application is similar to the geometric and operating parameters mentioned in table 5.2.1 for these cases, then the new model can be used very accurately. However, if the test conditions are close to the cases 3 and 7 in table 5.2.1, it is recommended to use the Yu et al. (1995) model. For these cases the X30% of

the new model is almost 80% and hence the new model can only be recommended with caution in these cases. For cases 9,10 and 11 in table 5.2.1, it is seen that the new model does equally as well as the existing models of Cavallini et al. (1999) or Thome et al. (1997). Hence for similar applications, either of these three models can be used.

Table 5.2.1. Specific applications studied for CO<sub>2</sub>

Case number	Tsat (°C)	D (mm)	G (kg/m <sup>2</sup> s)	q (W/m <sup>2</sup> )
1	10	4.4	212	16000
2	0	4.4	424	6000
3	5	4.4	424	20000
4	10	8.92	656	16000
5	-5	4.5	318	15000
6	15	1.996	360	4500
7	15	1.996	720	18000
8	10	3.04	380	20000
9	0	4.5	212	30000
10	5	8.62	250	4100
11	5	8.62	250	59900

The following graphs show individual datasets for CO<sub>2</sub>. The best existing model and the new linearized model can be compared with the experimental data. Trends of the experimental and predicted values can be seen from these graphs. From the graphs it is clear that the new linearized model is superior to the best from the existing model. From these trends for CO<sub>2</sub> it is also seen that for vapor qualities > 0.7 the new model slightly over-predicts the data while for vapor qualities < 0.4 the new model slightly under-predicts the data. The percentage deviations for any of these cases is not more than ± 30%. In general, for medium to high G (~ 500-700 kg/m<sup>2</sup>s) applications and medium q (around

20000 W/m<sup>2</sup>) applications with small diameters (<5mm) and T<sub>sat</sub>>0°C the Yu et al. (1995) correlation is recommended. For all other applications, the new model is recommended.

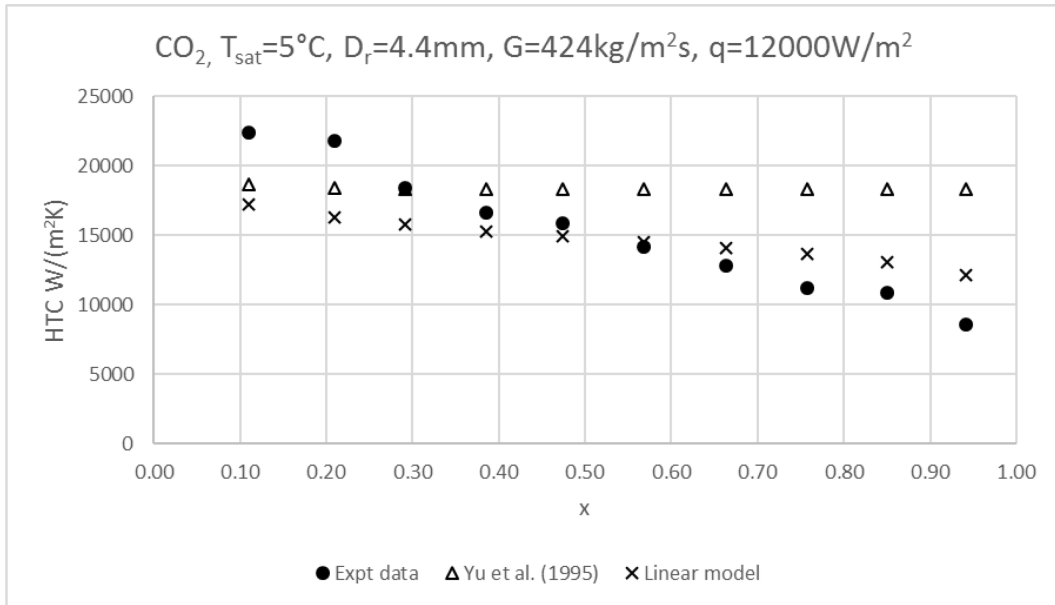


Figure 5.2.1. Comparison of trends for specific applications [ $CO_2$ ,  $T_{sat}=5^\circ C$ ,  $d_r=4.4mm$ ,  $G=424kg/m^2s$ ,  $q=12000W/m^2$ ] for linearized model and best among existing models

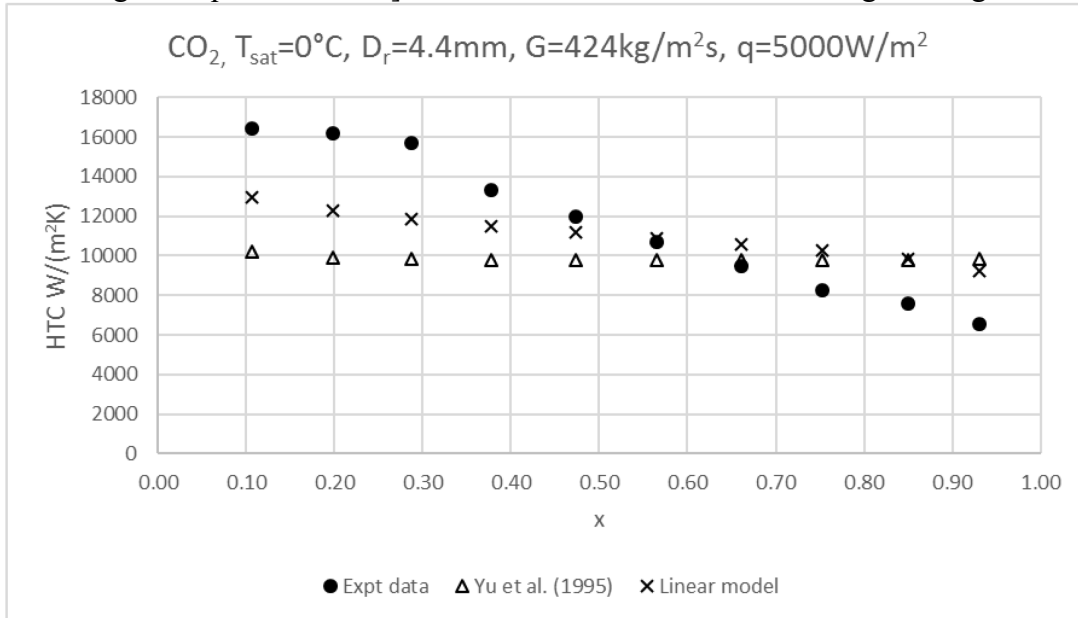


Figure 5.2.2. Comparison of trends for specific applications [ $CO_2$ ,  $T_{sat}=0^\circ C$ ,  $d_r=4.4mm$ ,  $G=424kg/m^2s$ ,  $q=5000W/m^2$ ] for linearized model and best among existing models

In existing literature there is no model specifically to predict flow boiling HTC's for Ammonia. Ammonia is a natural refrigerant and is gaining popularity due to slowly phasing out of man-made refrigerants that have high global warming potential. The new linearized model can be used for Ammonia with the set of recommended constants. In published literature, there is not much flow boiling experimental data reported for Ammonia. Kabelac and Buhr (2001) have reported flow boiling Ammonia data which has been used to derive the constants proposed in table 4.1.

Due to limited experimental data available for Ammonia, three cases of different operating parameters were studied for Ammonia. The cases are listed in table 5.2.2. For all the three cases studied the new model is clearly superior to the best of the existing models. Hence, for Ammonia refrigerant with geometric and operating parameters similar to the cases shown in table 3, the new model can be recommended with good accuracy. From the trend plot shown in Figure 5.2.3, it is seen that the trend of the experimental points is closely captured by the new linear model. At low quality < 20% the data is slightly over-predicted for Ammonia. Maximum percentage deviation is +20%

Table 5.2.2. Specific applications studied for Ammonia

Case number	Tsat (°C)	D (mm)	G (kg/m <sup>2</sup> s)	q (W/m <sup>2</sup> )
1	-20	11.13	50	50000
2	-20	11.13	100	50000
3	-20	11.13	150	40000

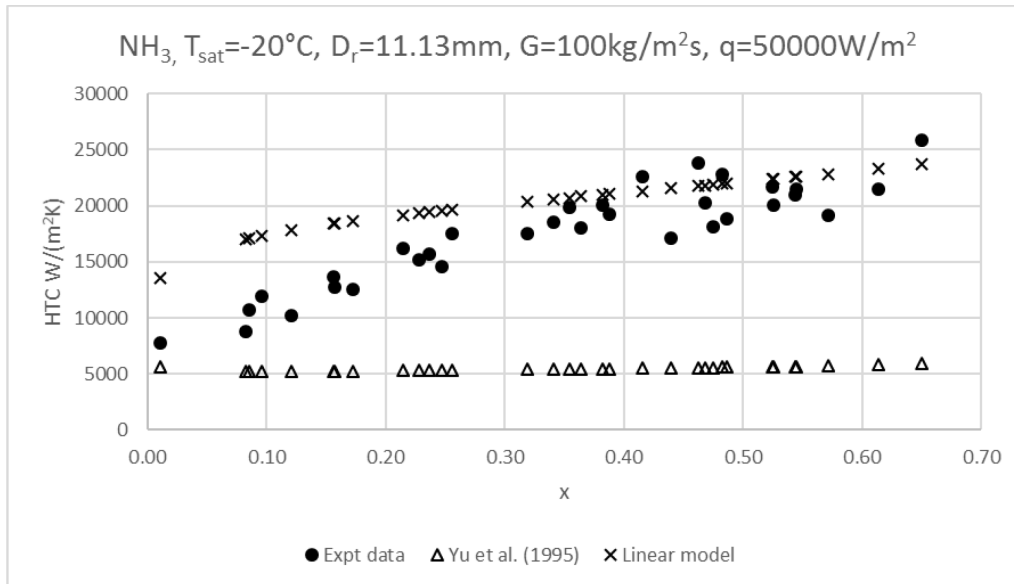


Figure 5.2.3. Comparison of trends for specific applications [ $\text{NH}_3, T_{\text{sat}} = -20^\circ\text{C}, d_r = 11.13\text{mm}, G = 100\text{kg/m}^2\text{s}, q = 50000\text{W/m}^2$ ] for linearized model and best among existing models

For halogenated refrigerants the 30 cases (table 5.2.3) were studied. For all cases (except case numbers 5, 10 and 25) the new model is superior to the existing models. Hence, if the practicing engineers are trying to model cases similar to these, it is recommended to use the new model to predict HTCs accurately. For cases 5, 10 and 25 it is recommended to use the Hamilton et al. (2008) model. However, even the Hamilton et al. (2008) model shows average X30% of 78% for these cases. Hence, even the Hamilton et al. (2008) model is recommended with caution. It is seen that for cases 5, 10 and 25 the new model follows the trends closely with X30% of about 75%. Hence, the new model is not very poor if compared to the best of the existing models (i.e. Hamilton et al. (2008)). Figures 5.2.4-5.2.7 show the trend study for sample halogenated database. All the points studied in table 5.2.3 are given in the appendix.

Table 5.2.3. Specific applications studied for Halogenated refrigerants

Case number	Refrigerant	Tsat (°C)	D (mm)	G (kg/m <sup>2</sup> s)	q (W/m <sup>2</sup> )
1	R134A	-14.5000	8.92	53	2100
2	R134A	-14.5000	8.92	107	4200
3	R134a	5.0000	8.92	100	5000
4	R134a	5.0000	8.92	300	5000
5	R134a	5.0000	8.92	500	5000
6	R134A	30.0000	3.64	190	10000
7	R134A	30.0000	3.64	565	10000
8	R134A	30.0000	3.64	755	25000
9	R134A	30.0000	3.64	755	50000
10	R134A	31.0000	8.15	80	14700
11	R134A	30.3000	8.15	400	28500
12	R134A	15.0000	8.92	800	10000
13	R134A	5	8.96	250	12500
14	R22	22.0000	14.85	225	14200
15	R22	15.0000	8.82	210	11000
16	R22	6.0400	8.92	200	6000
17	R32	10.0000	5.45	191	10000
18	R32	10.0000	5.45	382	10000
19	R32	9.787	5.37	400	15000
20	R1234ZE(e)	30.0000	3.64	190	10000
21	R1234ZE(e)	30.0000	3.64	375	25000
22	R1234ZE(e)	30.0000	3.64	375	50000
23	R1234ZE(e)	30.0000	3.64	755	25000
24	R407C	1.6600	8.92	200	6000
25	R407C	1.6600	8.92	200	14000
26	R407C	-10	8.95	300	1000
27	R407C	5	8.96	250	12500
28	R410A	15.0000	8.8	210	11000
29	R410A	30.1000	8.15	600	44200
30	R410A	30.3000	8.15	200	44100



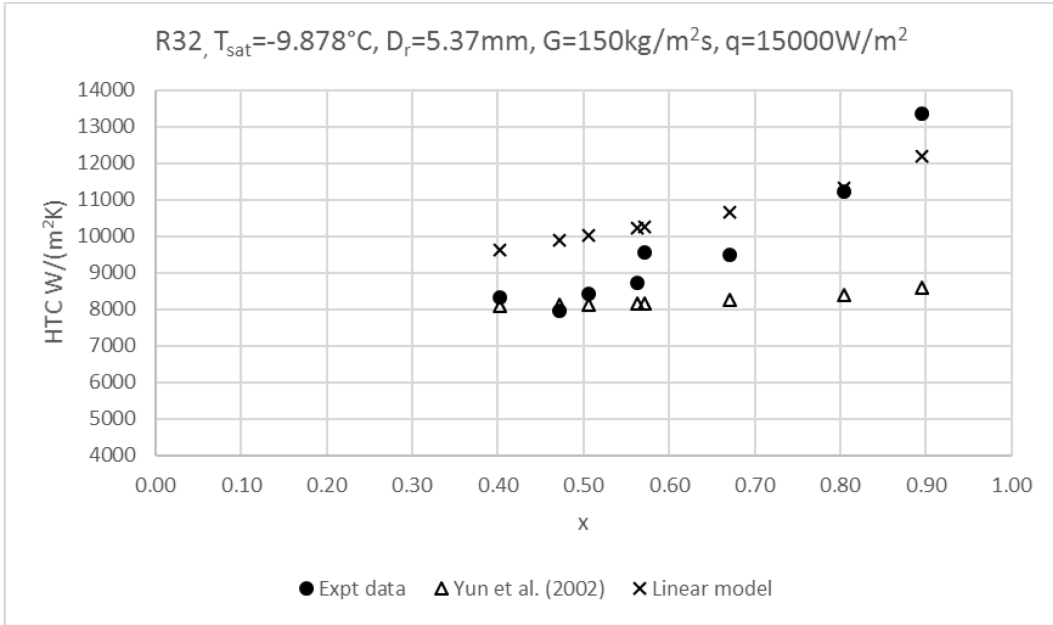


Figure 5.2.4. Comparison of trends for specific applications [R32,  $T_{sat} = -9.878^\circ\text{C}$ ,  $d_r = 5.37\text{mm}$ ,  $G = 150\text{kg/m}^2\text{s}$ ,  $q = 15000\text{W/m}^2$ ] for linearized model and best among existing models

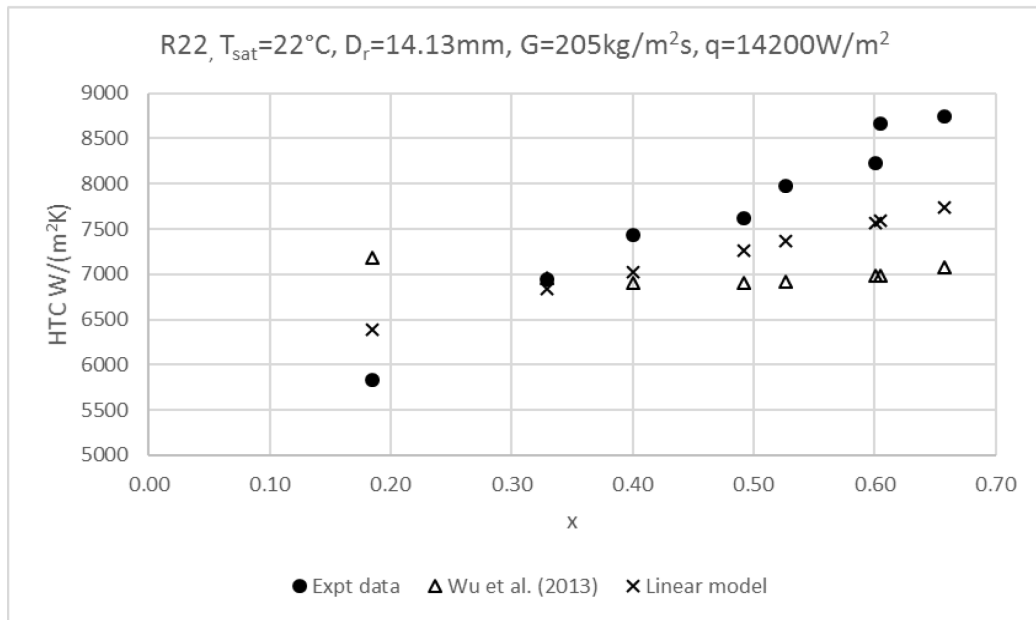


Figure 5.2.5. Comparison of trends for specific applications [R22,  $T_{sat} = 22^\circ\text{C}$ ,  $d_r = 14.13\text{mm}$ ,  $G = 205\text{kg/m}^2\text{s}$ ,  $q = 14200\text{W/m}^2$ ] for linearized model and best among existing models

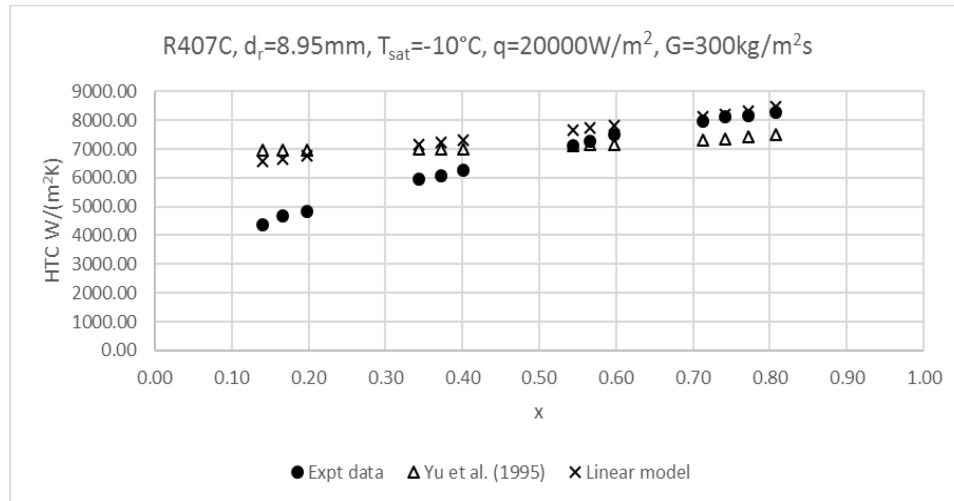


Figure 5.2.6. Comparison of trends for specific applications [R407C,  $T_{\text{sat}}=-10^\circ\text{C}$ ,  $d_r=8.95\text{mm}$ ,  $G=300\text{kg/m}^2\text{s}$ ,  $q=20000\text{W/m}^2$ ] for linearized model and best among existing models

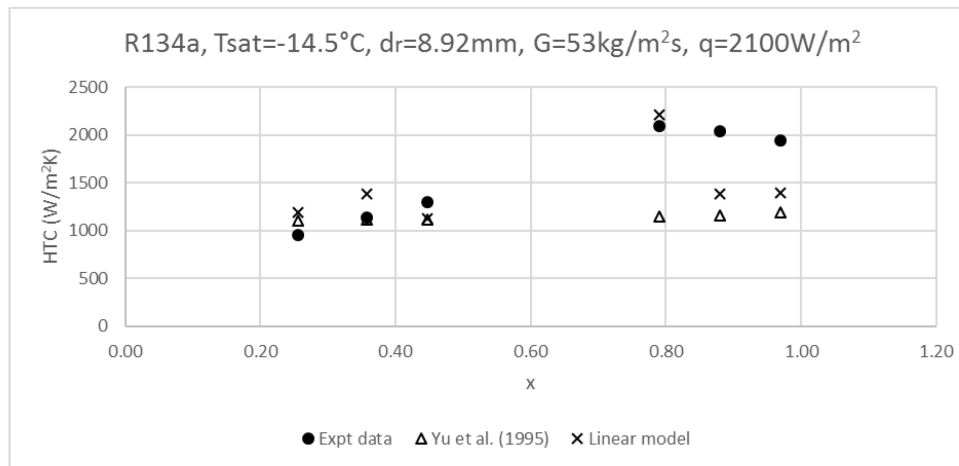


Figure 5.2.7. Comparison of trends for specific applications [R134a,  $T_{\text{sat}}=-14.5^\circ\text{C}$ ,  $d_r=8.92\text{mm}$ ,  $G=53\text{kg/m}^2\text{s}$ ,  $q=2100\text{W/m}^2$ ] for linearized model and best among existing models

General guidelines for halogenated refrigerants are given as follows-

- For R134a, with medium  $T_{\text{sat}}$  ( $5^\circ\text{C}$ ) and medium  $G$  ( $500\text{ kg/m}^2\text{s}$ ) the Hamilton et al. (2008) model is recommended with caution ( $X_{30\%}\sim 78\%$ )
- For R134a, with high  $T_{\text{sat}}$  ( $31^\circ\text{C}$ ) and low  $G$  ( $80\text{ kg/m}^2\text{s}$ ) the Hamilton et al. (2008) model is recommended with caution

- For R407C, with medium  $T_{sat}$  ( $1^{\circ}\text{C}$ ) and low  $G$  ( $200 \text{ kg/ m}^2\text{s}$ ) the Hamilton et al. (2008) model is recommended with caution
- Remaining all cases with other refrigerants the new model is recommended

In order to have fair comparison with the existing correlations, a sample test was conducted using Wu et al. (2013) correlation. For this comparison, the experimental database was replicated similar to the Wu et al. (2013) points. Experimental points that were used by Wu et al. (2013) were collected. Even though the exact same points could not be collected, an attempt was made to replicate the database as closely as possible. It was not possible to replicate the database exactly due to non-availability of papers and it was also observed that Wu et al. (2013) did not consider all points from the reference publications (Merchant and Mehendale (2015)). With the similar database collected the new model was run using R software to obtain coefficients for the database similar to Wu et al. (2013). Thus, the functional form of the equation remained as given by equation (4.1) but the experiments were similar to those studied by Wu et al. (2013). This functional form as proposed by equation (4.1) with the modified Wu et al. (2013) database was compared with the results obtained from the new model.

Table 5.2.4. Comparison of X30% for the modified Wu et al. (2013) and new model

X30%	Modified Wu et al. (2013) model	Linear model
Full data	70.45045	76.5
Halogenated ref.	75.41322	76.9
Carbon Dioxide	36.61972	77.4
Ammonia	N/A	61.7

From both these modes of Comparisons of X30% and trends, it was seen that the new model was superior to Wu et al. (2013). This exercise was conducted in order to have fair comparison between the correlations being studied and the new correlation.

As reported above, the linearized model proposed can predict flow boiling HTC's with greater confidence as compared to the existing models. In addition, the existing models only report MD, MAD and SD for the overall datasets. No existing model reports data for individual datasets or provides any application-specific guidelines to practicing engineers. The new model provides recommendations to the engineers based on trend studies. This is a novel contribution of this research aimed to aid the practicing engineer.

## 6. Conclusions and recommendations for future research

In published literature, there are many models to predict the flow boiling HTC in microfin tubes. Flow boiling in microfin tubes is a complex phenomenon involving the interplay of many parameters. Hence, mathematical models proposed are empirical or semi-empirical. It has been observed that no single model can predict flow boiling HTC over the entire range of data. Hence the practicing engineer often faces the task of selecting the most accurate model to predict experimental data. Due to the lack of clear guidance, the engineers have to resort to costly and time consuming experimentation. In order to reduce this time and cost it is important to have models to predict the flow boiling HTC data. In the current work, a linearized model is proposed to predict flow boiling HTC data spanning over a wide range of refrigerants, geometric and operating parameters. This linearized model is the first of its kind for Ammonia refrigerant. The experimental database is comprehensive consisting of 2201 data points from existing literature. The statistical parameters like MD, MAD, SD and X30%, do not provide specific guidelines for industrial applications. Hence, in the current work, recommendations have been provided for the models to be used based on their applicability to specific cases. The new linearized model can be used to predict HTC data accurately. Based on the current work, it is seen that the experimental database considered is crucial to determine the empirical constants. Hence, more experiments added to the database will make the work more robust. In addition, an asymptotic model that captures the physics of convective and nucleate boiling may increase the ability of the model to predict flow boiling data accurately.

## References

Akhavan-Behabadi, M., Mohseni, S. and Razavinasab, S., 2011. "Evaporation Heat Transfer of R-134a Inside a Microfin Tube with Different Tube Inclinations," *Experimental Thermal and Fluid Science*, 35(6), pp. 996-1001.

Baba, D., Nakagawa, T., Koyama, S., 2012, "Flow Boiling Heat Transfer and Pressure Drop of R1234ze(E) and R32 in a Horizontal Micro-Fin tube." *International Refrigeration and Air Conditioning Conference*, pp. 1218

Bandarra Filho, E. and Barbieri, P., 2011, "Flow Boiling Performance in Horizontal Micro Finned Copper Tubes with The Same Geometric Characteristics." *Experimental Thermal and Fluid Science*, 35(5), pp. 832-840.

Bandarra Filho, E. and Saiz Jabardo, J., 2006. "Convective Boiling Performance of Refrigerant R-134a in Herringbone and Microfin Copper Tubes." *International Journal of Refrigeration*, 29(1), pp.81-91.

Cavallini, A., Del Col, D., Doretti L., Longo, G.A., Rosetto, L., 1999, "Enhanced in Tube Heat Transfer with Refrigerants", in: *Proceedings of the 20th International Congress of Refrigeration, IIR/IIF, Sydney, Australia*, 2, pp. 731.

Cavallini, A., Del Col, D., Doretti L., Longo, G.A., Rosetto, L., 1999, "Refrigerant Vaporization Inside Enhanced Tubes: A Heat Transfer Model", *Heat and Technology*, 17(2), pp. 29-36.

Chamra, L. and Mago, P., 2007, "Modelling of Evaporation Heat Transfer of Pure Refrigerants and Refrigerant Mixtures in Microfin Tubes." Proceedings of the Institution of Mechanical Engineers, Part C: Journal of Mechanical Engineering Science, 221(4), pp. 443-447.

Chamra, L. and Webb, R. 1995, "Condensation and Evaporation in Micro-Fin Tubes at Equal Saturation Temperatures." Journal of Enhanced Heat Transfer, 2(3), pp. 219-229.

Chamra, L., Tan, M., Kung, C. and Tang, S. 2003, "Evaluation of Existing Evaporative Heat-Transfer Models in Horizontal Microfin Tubes." In: Symposium, ASHRAE Transactions, vol. 109, pt. 1.

Cho, J. and Kim, M., 2007, "Experimental Studies On the Evaporative Heat Transfer and Pressure Drop of CO<sub>2</sub> in Smooth and Micro-Fin Tubes of the Diameters of 5 And 9.52 mm." International Journal of Refrigeration, 30(6), pp. 986-994.

Cooper, M.G., 1984, "Heat Flows Rates in Saturated Pool Boiling – A Wide Ranging Examination Using Reduced Properties." Advanced in Heat Transfer, Academic Press, Orlando, Florida, pp. 157-239.

Dang, C., Haraguchi, N. and Hihara, E., 2010, "Flow Boiling Heat Transfer of Carbon Dioxide Inside a Small-Sized Microfin Tube." International Journal of Refrigeration, 33(4), pp. 655-663.

Del Col, D., Webb, R. and Narayanamurthy, R., 2002, "Heat Transfer Mechanisms for Condensation and Vaporization Inside a Microfin Tube." *Journal of Enhanced Heat Transfer*, 9(1), pp. 25-37.

Diani, A., Mancin, S. and Rossetto, L., 2014, "R1234ze(E) Flow Boiling Inside A 3.4 mm ID Microfin Tube." *International Journal of Refrigeration*, 47, pp. 105-119.

Eckels, S., Doerr, T.M., and Pate, M., 1991, "In-Tube Heat Transfer and Pressure Drop of R-134A and Ester Lubricant Mixtures in A Smooth Tube and A Micro-Fin Tube: Part 1- Evaporation." *ASHRAE transactions: Research*, pp. 265-282.

Fujie, K., Itoh, N., Innami, T., Kimura, H., Nakayama, N., and Yanugidi, T., 1977, "Heat Transfer Pipe," U.S Patent 4,044,797, assigned to Hitachi Ltd.

Gao, L., Honda, T. and Koyama, S., 2007, "Experiments on Flow Boiling Heat Transfer of Almost Pure CO<sub>2</sub> and CO<sub>2</sub>-Oil Mixtures in Horizontal Smooth and Microfin Tubes." *HVAC&R Research* 13(3), pp. 415-425.

Hu, H., Ding, G. and Wang, K., 2008, "Heat Transfer Characteristics of R410A–Oil Mixture Flow Boiling Inside A 7 mm Straight Microfin Tube." *International Journal of Refrigeration*, 31(6), pp. 1081-1093.

Jiang, G.B., Tan, J.T., Q.X. Nian, Q. X., Tang, S.C., Tao, W.Q., 2016, "Experimental Study of Boiling Heat Transfer in Smooth/Micro-Fin Tubes of Four Refrigerants" *International Journal of Heat and Mass Transfer*, 98, pp. 631–642



Jung D. S., Radermacher R., 1990, "Performance Evaluation of Pure and Mixed Refrigerants in Domestic Refrigerators: Drop-in Replacement of R12" International Refrigeration and Air Conditioning Conference. Paper 100.

Kabelac, S., Buhr, H.J., 2001, "Flow Boiling of Ammonia in a Plain and Low Finned Horizontal Tube" International Journal of Refrigeration, 24, pp. 41-50.

Kandlikar, S. and Raykoff, T., 1997, "Predicting Flow Boiling Heat Transfer of Refrigerants in Microfin Tubes." Journal of Enhanced Heat Transfer, 4(4), pp. 257-268.

Kandlikar, S., 1991, "A Model for Correlating Flow Boiling Heat Transfer in Augmented Tubes and Compact Evaporators." Journal of Heat Transfer, 113(4), p. 966.

Kandlikar, S., 1999, "Handbook of Phase Change: Boiling and Condensation." CRC Press.

Kattan, N., Thome J.R., and Favrat D., 1998c, "Flow Boiling in Horizontal Tubes: Part 3—Development of A New Heat Transfer Model Based On Flow Pattern." ASME J. Heat Transfer 120: 156-165.

Kido O. and Uehara H., 1994, Trans. of the JAR, 11(2), pp.730

Kim, M. and Shin, J., 2005, "Evaporating Heat Transfer of R22 and R410A in Horizontal Smooth and Microfin Tubes." International Journal of Refrigeration, 28(6), pp. 940-948.

Kim, Y., Cho, J. and Kim, M., 2008, "Experimental Study On the Evaporative Heat Transfer and Pressure Drop of CO<sub>2</sub> Flowing Upward in Vertical Smooth and Micro-Fin

Tubes with The Diameter of 5 mm.” International Journal of Refrigeration, 31(5), pp. 771-779.

Kimura, H. and Ito, M., 1981, “Evaporating Heat Transfer in Horizontal Internal Spiral-grooved Tubes in the Region of Low Flow Rates.” Bulletin of JSME, 24(195), pp.1602-1607.

Kondou, C., BaBa, D., Mishima, F. and Koyama, S., 2013, “Flow Boiling of Non-Azeotropic Mixture R32/R1234ze(E) In Horizontal Microfin Tubes.” International Journal of Refrigeration, 36(8), pp. 2366-2378.

Koyama S., Yu J., Momoki S., Fujii T. and Honda H., 1995, Proceedings of International Conference on Convective Flow Boiling, Banff, Canada, IV-3.

Kuo, C. and Wang, C., 1996, “In-Tube Evaporation of HCFC-22 In A 9.52 mm Micro-Fin/Smooth Tube.” International Journal of Heat and Mass Transfer, 39(12), pp. 2559-2569.

Mancin, S., Diani, A. and Rossetto, L., 2014, “Experimental Measurements of R134a Flow Boiling Inside a 3.4 mm ID Microfin Tube.” Heat Transfer Engineering, 36(14-15), pp. 1218-1229.

Mehendale, S., 2013, “The Impact of Fin Deformation On Condensation Heat Transfer Coefficients in Internally Grooved Tubes” Paper No. HT2013-17111, pp. V002T07A002; doi: 10.1115/HT2013-17111, ASME 2013 Summer Heat Transfer Conference, Minneapolis, MN, USA, July 14–19, 2013.

Merchant, R. and Mehendale, S. S., 2015. "Application-Based Methodology for Assessment of Flow Boiling Correlations in Microfin Tubes." ASME 2015 International Mechanical Engineering Congress and Exposition (IMECE), Houston, TX, USA

Miyara A., Koyama S., Takamatsu H., Yonemoto K. and Fujii T., 1988, "Condensation and Evaporation of Nonazeotropic Refrigerant Mixtures of R22 and R114 inside a Spirally Grooved Horizontal Tube." The Reports of Institute of Advanced Material Study, Kyushu University, Vol.1, No.1, pp.57-75(in Japanese).

Murata, K. and Hashizume, K., 1993, "Forced Convective Boiling of Nonazeotropic Refrigerant Mixtures Inside Tubes.", Journal of Heat Transfer, 115(3), pp.680.

Padovan, A., "Experimental Study On Flow Boiling of Refrigerants Inside Horizontal Tubes." Ph.D. Thesis, Università Degli Studi di Padova.

Padovan, A., "Experimental Study On Flow Boiling of Refrigerants Inside Horizontal Tubes" Thesis: Università Degli Studi Di Padova

Padovan, A., Del Col, D. and Rossetto, L., 2011, "Experimental Study On Flow Boiling of R134a and R410A in A Horizontal Microfin Tube at High Saturation Temperatures." Applied Thermal Engineering, 31(17-18), pp. 3814-3826.

Ravigururajan T.S., Bergles A.E., "General correlations for pressure drop and heat transfer for single-phase turbulent flow in internally ribbed tubes", Augmentation of Heat Transfer in Energy Systems, 52 (1985) 9–20 (ASME HTD).

Rollmann, P., Spindler, K., 2016, "New Models for Heat Transfer and Pressure Drop During Flow Boiling of R407C and R410A in A Horizontal Microfin Tube" International Journal of Thermal Sciences, 103, pp. 57-66

Rollmann, P., Spindler, K., Muller-Steinhagen, H., 2011, "Heat Transfer, Pressure Drop and Flow Patterns During Flow Boiling of R407C in A Horizontal Microfin Tube" Heat and mass transfer, 47, pp. 951-961

Rouhani, S. and Axelsson, E., 1970, "Calculation of Void Volume Fraction in The Subcooled and Quality Boiling Regions." International Journal of Heat and Mass Transfer, 13(2), pp. 383-393.

Schael, A. and Kind, M., 2005, "Flow Pattern and Heat Transfer Characteristics During Flow Boiling of CO<sub>2</sub> in A horizontal micro fin tube and comparison with smooth tube data." International Journal of Refrigeration, 28(8), pp. 1186-1195.

Spindler, K., Muller-Steinhagen, H., 2009, "Flow Boiling Heat Transfer of R134a and R404A in A Microfin Tube at Low Mass Fluxes and Low Heat Fluxes." Heat and mass transfer, 45, pp. 967-977

Steiner, D., 1993, "Heat Transfer to Boiling Saturated Liquids." VDI-Wärmeatlas.

Takamatsu, H., Momoki, S. and Fujii, T., 1993, "A Correlation for Forced Convective Boiling Heat Transfer of Pure Refrigerants in A Horizontal Smooth Tube." International Journal of Heat and Mass Transfer, 37(9), pp. 1421.

Thome J., 1997, "Heat transfer and pressure drop in the dry-out region of in-tube evaporation with refrigerant/lubricant mixtures", ASHRAE Final Report RP-800.

Wedekind, G.L., 1965, "Transient Response of the Mixture-Vapor Transition Point in Two-Phase Horizontal Evaporating Flow." Ph.D. Thesis, University of Illinois at Urbana-Champaign.

Wongsa-ngam, J., Nualboonrueng, T. and Wongwises, S., 2002, "Performance of Smooth and Micro-Fin Tubes in High Mass Fluxes Region of R-134a During Evaporation." Heat and Mass Transfer, 40(6-7), pp. 425-435.

Wu, Z., Sundén, B., Wadekar, V. and Li, W., 2014. "Heat Transfer Correlations for Single-Phase Flow, Condensation, and Boiling in Microfin Tubes." Heat Transfer Engineering, 36(6), pp. 582-595.

Wu, Z., Wu, Y., Sundén, B. and Li, W., 2013, "Convective Vaporization in Micro-Fin Tubes of Different Geometries." Experimental Thermal and Fluid Science, 44, pp. 398-408.

Yu, J., Koyama, S. and Momoki, S., 1995, "Experimental Study of Flow Boiling in a Horizontal Microfin Heat Transfer Tube." Kyushu University, Vol, 9, No, 1.

Yun, R., Kim, Y., Seo, K. and Young Kim, H., 2002, "A Generalized Correlation for Evaporation Heat Transfer of Refrigerants in Micro-Fin Tubes." International Journal of Heat and Mass Transfer, 45(10), pp. 2003-2010.

## Appendix A

